
ISS, August 2024

An Introduction to Space Environment Effects:
Spacecraft Charging

Joseph I. Minow
Technical Fellow for Space Environments
NASA, Marshall Space Flight Center

EMA Expo
26 June 2025, virtual
joseph.minow@nasa.gov

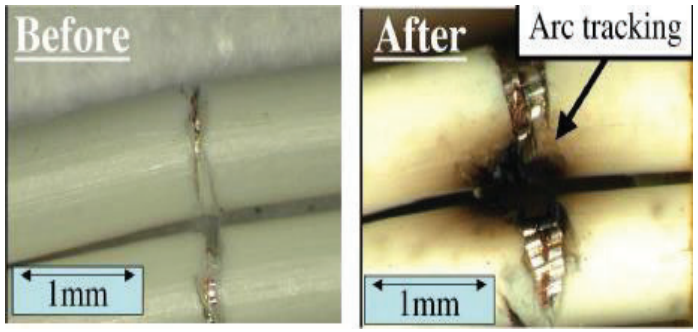
Spacecraft Charging Impacts Space Systems

Space Environment Impacts on Space Systems (Koons et al., 2000)

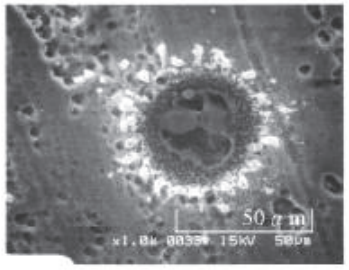
Anomaly Diagnosis	Number	%
ESD-Internal, Surface and uncatergorized	162	54.1
SEU (GCR, SPE, SAA, etc.)	85	28.4
Radiation Dose	16	5.4
Micrometeoroids, orbital debris	10	3.3
Atomic oxygen	1	0.3
Atmospheric drag	1	0.3
Other	24	8.0
Total	299	100.0%

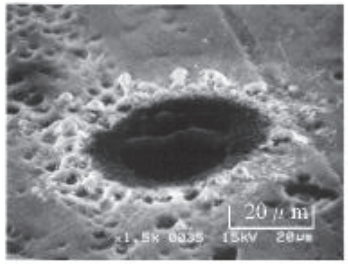
Risks to Spacecraft

- Phantom commands
- Discharge currents damage materials, electronics systems
- Damage to thermal control coatings, solar cells
- Trigger arcs on power systems lead to sustained arcing



Kawakita et al., 2005







Kawakita et al., 2005

Anomalies and Failures Attributed to Charging

Spacecraft	Year(s)	Orbit	Impact*	Spacecraft	Year(s)	Orbit	Impact*
DSCS II	1973	GEO	LOM	Intelsat K	1994	GEO	Anom
Voyager 1	1979	Jupiter	Anom	DMSP F13	1995	LEO	Anom
SCATHA	1982	GEO	Anom	Telstar 401	1994, 1997	GEO	Anom/LOM
GOES 4	1982	GEO	LOM	TSS-1R	1996	LEO	Failure
AUSSAT-A1, -A2, -A3	1986-1990	GEO	Anom	TDRS F-1	1986-1988	GEO	Anom
FLTSATCOM 6071	1987	GEO	Anom	TDRS F-3,F-4	1998-1989	GEO	Anom
GOES 7	1987-1989	GEO	Anom/SF	INSAT 2	1997	GEO	Anom/LOM
Feng Yun 1A	1988	LEO	Anom/LOM	Tempo-2	1997	GEO	LOM
MOP-1, -2	1989-1994	GEO	Anom	PAS-6	1997	GEO	LOM
GMS-4	1991	GEO	Anom	Feng Yun 1C	1999	LEO	Anom
BS-3A	1990	GEO	Anom	Landsat 7	1999-2003	LEO	Anom
MARECS A	1991	GEO	LOM	ADEOS-II	2003	LEO	LOM
Anik E1	1991	GEO	Anom/LOM	TC-1,2	2004	~2xGTO, GTO	Anom
Anik E2	1991	GEO	Anom	Galaxy 15	2010	GEO	Anom
Intelsat 511	1995	GEO	Anom	Echostar 129	2011	GEO	Anom
SAMPEX	1992-2001	LEO	Anom	Suomi NPP	2011-2014	LEO	Anom
				Intelsat 29e	2019	GEO	LOM

*Anom=anomaly SF=system failure LOM=Loss of mission

(Adapted from Spacecraft Anomalies and Failures Workshop, 24 July 2014)

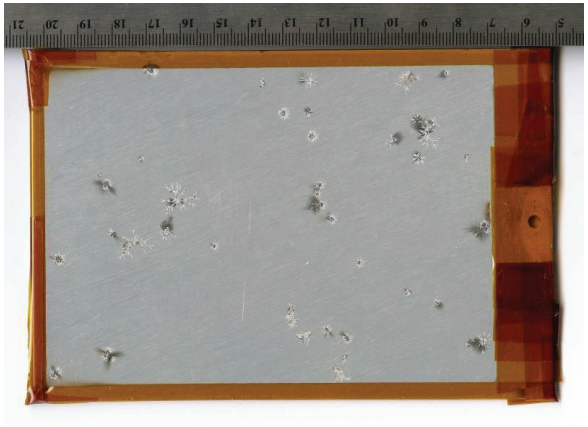
Mechanism for Charging Anomalies and Failures

- Accumulation of excess negative charge or inductive re-distribution of charge generates potential differences between spacecraft and space (frame potential) or between two points on the spacecraft (differential potential)

- An electrostatic discharge (ESD) results when electric fields associated with potential differences ($\mathbf{E} = -\nabla\Phi$) exceed the dielectric breakdown strength of materials allowing charge to flow in an arc
  - Typical dielectric breakdown strengths ~ 10^7 V/m to 10^8 V/m

- Damage depends on energy available to arc Energy = $\frac{1}{2}CV^2$

- Charging anomalies and failures depend on
  - Magnitudes of the induced potentials and strength of the electric fields
  - Material configuration and charge configuration (electrical capacitance)
  - Electrical properties of the materials
    - Surface and volume resistivity, dielectric constant
    - Secondary and backscattered electron yields, photoemission yields
    - Dielectric breakdown strength



ISS MMOD shield 1.3 μm chromic acid anodized thermal control coating. (T. Schneider/NASA)



PMMA (acrylic) charged by ~2 MeV to 5 MeV electrons



Impact of Charging on Spacecraft Systems

- Electrostatic discharge (ESD) currents
  - Compromised function and/or catastrophic destruction of sensitive electronics
  - Solar array string damage (power loss), solar array failures
  - Un-commanded change in system states (phantom commands)
  - Loss of synchronization in timing circuits
  - Spurious mode switching, power-on resets, erroneous sensor signals
  - Telemetry noise, loss of data

- Electromagnetic interference (EMI)
  - EMI noise levels in receiver band exceeding receiver sensitivity
  - Communications issues due to excess noise
  - Phantom commands, signals

- Material damage
  - ESD damage to mission critical materials including thermal control coatings, re-entry thermal protection systems, optical materials (dielectric coatings, mirror surfaces)
  - Re-attracted photoionized outgassing materials deposited as surface contaminants

- Other
  - Compromised science instruments, sensor functions
    - Modified “Ion line” charging signature in ion spectrum
    - Photoelectron contamination in electron spectrum
  - Parasitic currents and solar array power loss (LEO)

Potential Distributions on Spacecraft Surfaces

- **Electrostatic potentials**
  - Due to net charge density on spacecraft surfaces of or within insulating materials due to current collection to/from the space environment
  - Examples include
    - Plasma currents to surface
    - Secondary electron currents
    - Photoelectron currents
    - Solar array current collection
    - Active current sources (Electron, ion beams, electric thrusters, plasma contactors)
    - Energetic (~MeV) electrons
- **Electrodynamic (inductive) potentials**
  - Modification of frame potentials without change in net charge on spacecraft
  - Plasma environment not required
  - Examples include
    - EMF generated by motion of conductor through magnetic field
    - Externally applied electric fields

Surface charging

$$\frac{dQ}{dt} = C\frac{d\phi}{dt} = \sum_k I_k \quad \sim \mathbf{0\ at\ equilibrium}$$

Internal (deep dielectric) charging

$$\vec{\nabla}\cdot\vec{D} = \vec{\nabla}\cdot\varepsilon\vec{E} = \vec{\nabla}\cdot\varepsilon(-\vec{\nabla}\phi) = \rho$$

$$\nabla^2\phi = -\rho/\varepsilon$$

$$\frac{\partial\rho}{\partial t} = -\nabla\cdot J \quad \text{where } J = J_R + J_C$$

$$\vec{F} = q(\vec{E} + \vec{v}\times\vec{B}) \quad \text{Laboratory frame}$$

$$\vec{F}' = q\vec{E}' \quad \text{Spacecraft rest frame}$$

$$\vec{E}' = \vec{E} + \vec{v}\times\vec{B} \quad \text{Forces equal in both frames!}$$

$$\varepsilon'_m = \oint_C \vec{E}'\cdot d\vec{S} = \oint_C (\vec{E} + \vec{v}\times\vec{B})\cdot d\vec{S}$$

$$\Delta\phi' = \oint_C (\vec{E} + \vec{v}\times\vec{B})\cdot d\vec{S}$$

[c.f., *Whipple*, 1981; p. 272 *Wangness*, 1986; p. 210 *Jackson*, 1975; *Maynard*, 1998]

Surface Charging Current Balance

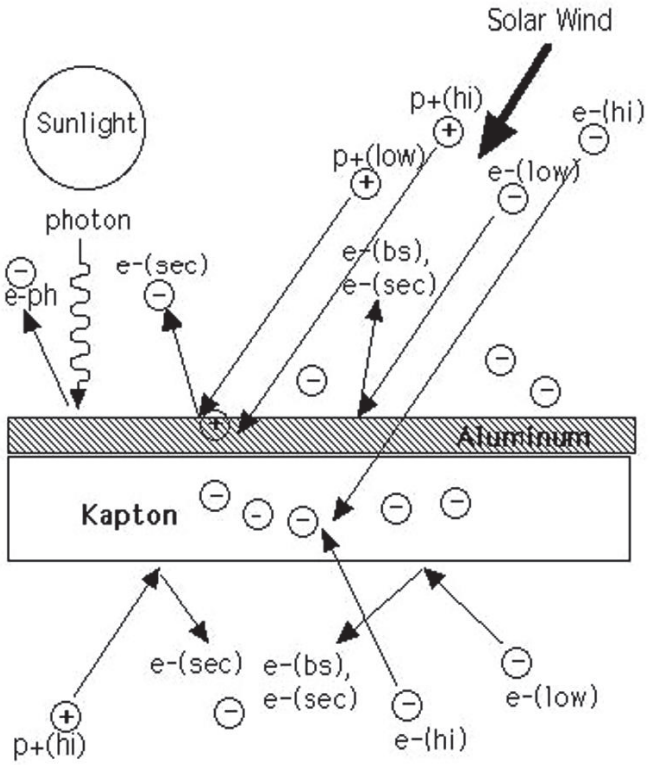
Time dependent current balance

$$\frac{dQ}{dt} = \frac{d\sigma}{dt} A = C \frac{dV}{dt} = \sum_k I_k = 0$$ at equilibrium

Currents

$$\frac{dQ}{dt} = \sum_k I_k =$$

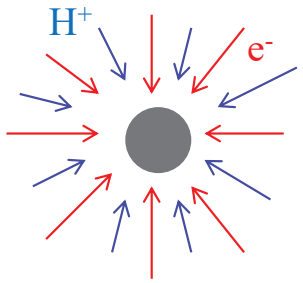
$+ I_i(V)$	**incident ions**
$- I_e(V)$	**incident electrons**
$+ I_{bs,e}(V)$	**backscattered electrons**
$+ I_c(V)$	**conduction currents**
$+ I_{se}(V)$	**secondary electrons due to I_e**
$+ I_{si}(V)$	**secondary electrons due to I_i**
$+ I_{ph,e}(V)$	**photoelectrons**
$+ I_b(V)$	**active current sources (beams, thrusters)**



[Garrett and Minow, 2004]

Simple Satellite Surface Charging Potential Analysis

- Example, let's derive the equation for the potential of a stationary, passive conducting object: balance the electron and ion fluxes and assume the election and ion temperatures are the same (neglect photoelectrons)



  - Mean speed of the particles in a plasma is given by $u_{o,\alpha} = \sqrt{\frac{8kT_\alpha}{\pi m_\alpha}}$
    - u = mean speed
    - α = species (electron or ion)
    - k = Boltzmann's constant
    - T = temperature

- Flux (particles per unit area per unit time crossing a surface) is given by $\Gamma_\alpha = \frac{n_o u_\alpha}{4}$

- The electron density is given by $n_{e,i} = n_o \exp\left(\frac{e\Phi}{kT_{e,i}}\right)$

  (This represents the electron density at the surface of a conducting object charged to Φ. In a space plasma in darkness, $\Phi < 0$, so n_e will be less than the ambient plasma density n_o)

- Set the electron flux = ion flux $n_e \exp\left(\frac{e\Phi}{kT_e}\right)\sqrt{\frac{8kT_e}{\pi m_e}} = n_i\sqrt{\frac{8kT_i}{\pi m_i}}$

Simple Satellite Surface Charging Potential Analysis

- Solve for potential at equilibrium, $n_e \sim n_i$

$$\phi = -\frac{kT_e}{e} \ln\left[\left(\frac{T_e}{T_i}\frac{m_i}{m_e}\right)^{1/2} \frac{n_e}{n_i}\right]$$

LEO O^+ plasma with $kT_e \sim kT_i \sim 0.1$ eV (ISS daytime)

$$\phi \sim -\frac{kT_e}{e} 5.13 \quad \sim 0.5 \text{ volt}$$

LEO H^+ plasma with $kT_e \sim kT_i \sim 1$ keV (auroral zone)

$$\phi \sim -\frac{kT_e}{e} 3.74 \quad \sim 3700 \text{ volts}$$

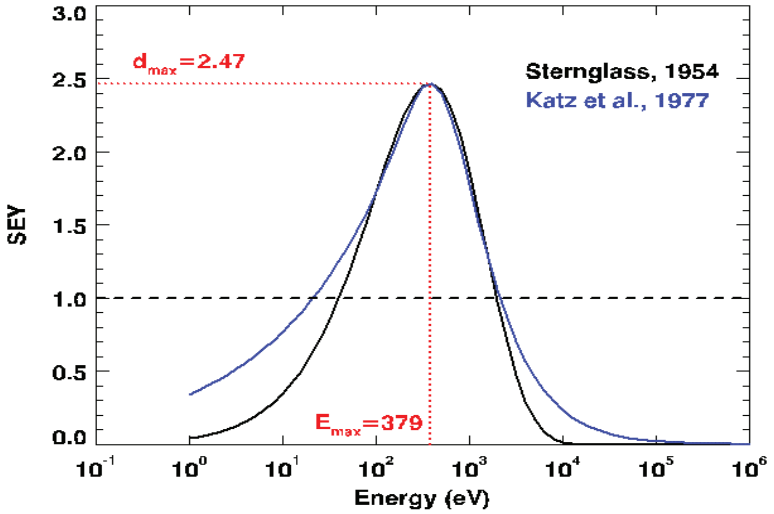
GEO H+ plasma with $kT_e \sim 16$ keV (geomagnetic storm)
$kT_i \sim 28$ keV

$$\phi \sim -\frac{kT_e}{e} 3.47 \quad \sim 55{,}500 \text{ volts}$$

- Neglects
  - Secondary electron emission (best for high energy electrons)
  - Photoemission (spacecraft in darkness)
  - Ram flux (environments dominated by hot electrons, ions with thermal speed that exceeds spacecraft velocity)

- Closed form potential solution provides convenient technique for rapid screening of large sets of plasma moments
  - Preserves N-T correlations
  - Not intended to provide quantitative computation of spacecraft potential

Secondary Electron Yields



$$\frac{dQ}{dt} = \sum_k I_k = +I_i - I_e + I_{se} + I_{ph,e}$$
$$= +I_i - I_e(1-\delta) + I_{ph,e}$$

$$\delta_e(E,\theta) = \delta_{e,\max} \frac{E}{E_{\max}} \exp\left(2 - 2\sqrt{E/E_{\max}}\right) \exp[2(1-\cos\theta)]$$

Sternglass, 1954

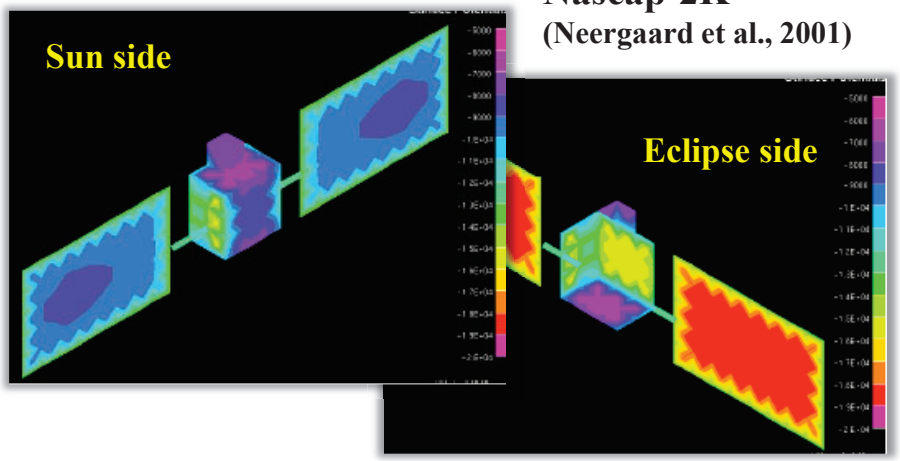
$$\delta_e(E,\theta) = \frac{1.114\delta_{e,\max}}{\cos\theta}\left[\frac{E}{E_{\max}}\right]^{0.35}\left\{1 - \exp\left[-2.28\cos\theta\left[\frac{E_{\max}}{E}\right]^{1.35}\right]\right\}$$

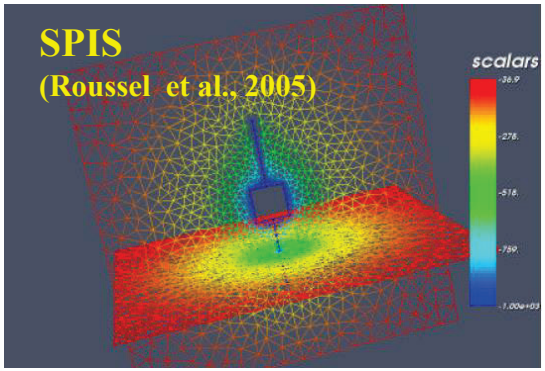
Katz et al., 1977

Whipple, 1981

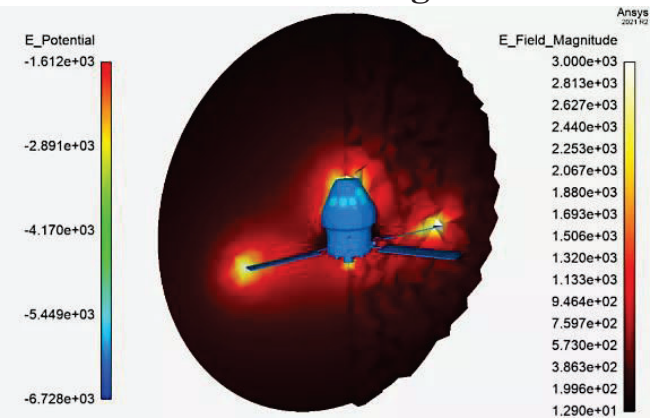
3-D Surface Charging Models

Nascap-2K
(Neergaard et al., 2001)

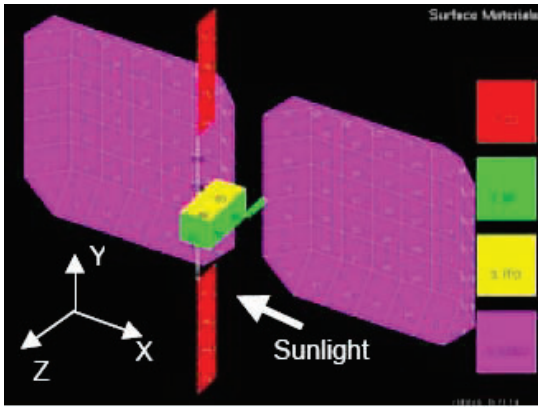


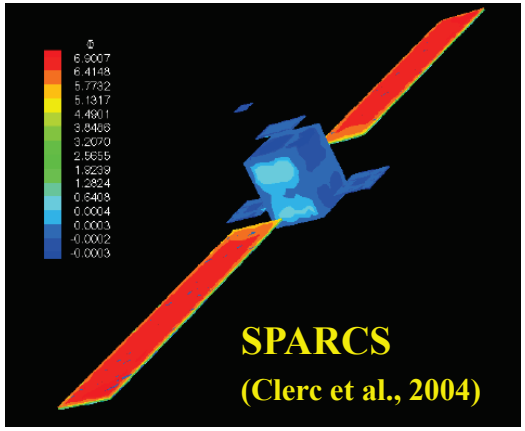


EMA3D Charge Plus

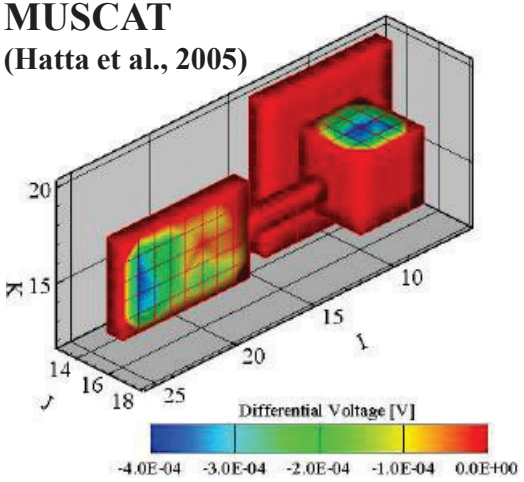


NASCAP/GEO
(Fuji et al., 2001)





MUSCAT
(Hatta et al., 2005)



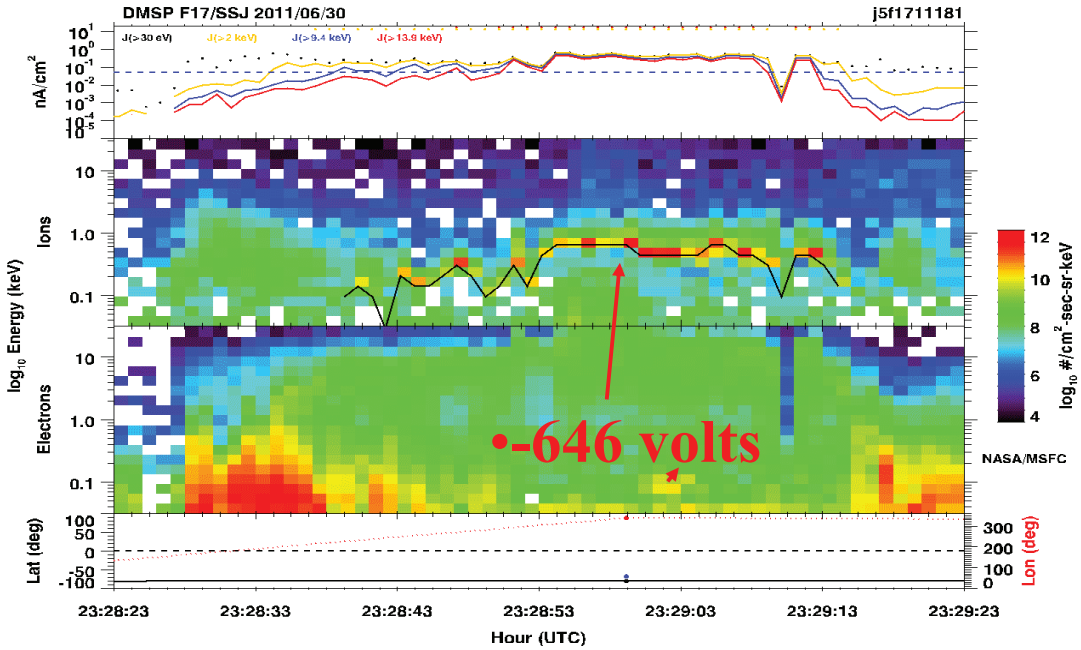
Ion-line Charging Signature

- Low energy background ions accelerated by spacecraft potential show up as sharp “line” of high ion flux in single channel of electrostatic ion analyzer records

$$E = E_0 + q\Phi$$

- Thermal ion temperature is ~0.1 eV at DMSP altitudes so we can set $E_0 \sim 0$ for single charged ionospheric ions (O^+, H^+) and read the spacecraft frame potential (volts) directly from ion line energy in electron volts (eV)

- DMSP SSJ4, SSJ5 electrostatic analyzers
  - Electrons: 20 channels
    30 eV to 30 keV
  - Ions: 20 channels
    30 eV to 30 keV

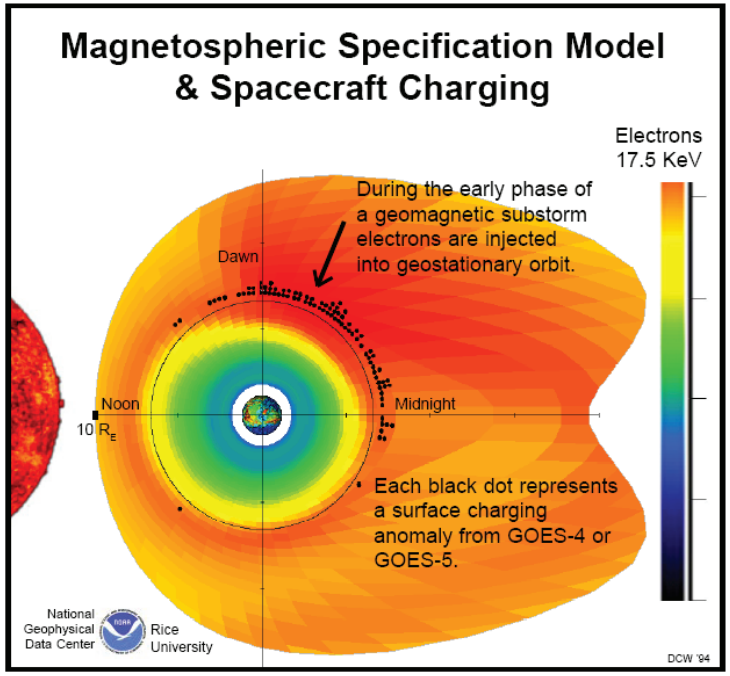


DMSP SSJ/4 and SSJ/5 Nominal Ion Energy Channels

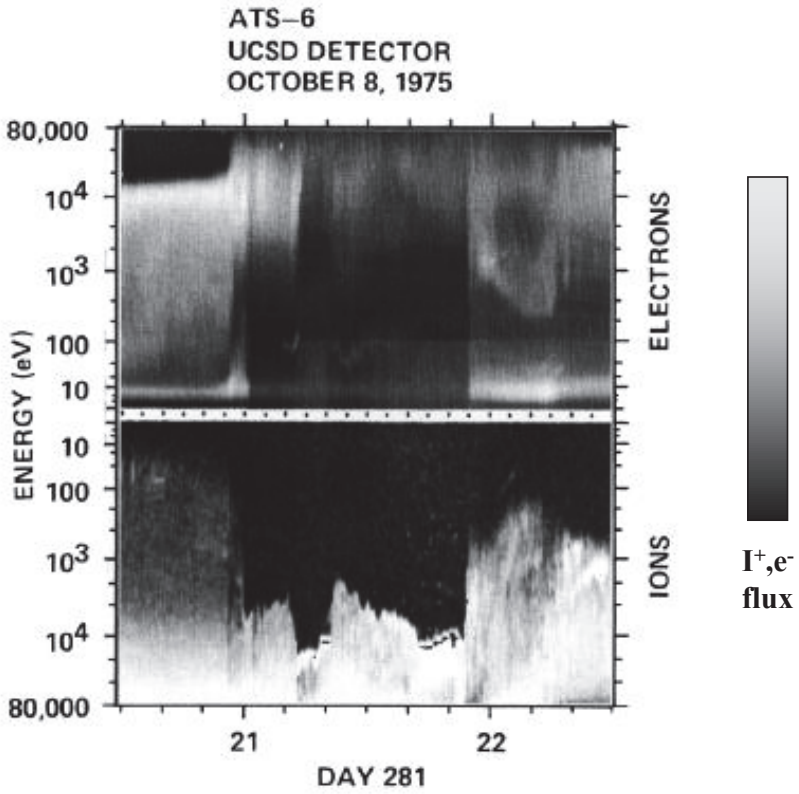
Channel	0	1	2	3	4	5	6	7	8	9
Energy (eV)	30	44	65	95	139	204	300	440	646	949
Channel	10	11	12	13	14	15	16	17	18	19
Energy (eV)	949	1,392	2,040	3,000	4,400	6,460	9,450	13,900	20,400	30,000

$\Delta E/E \sim 9\%$

GEO Surface Charging



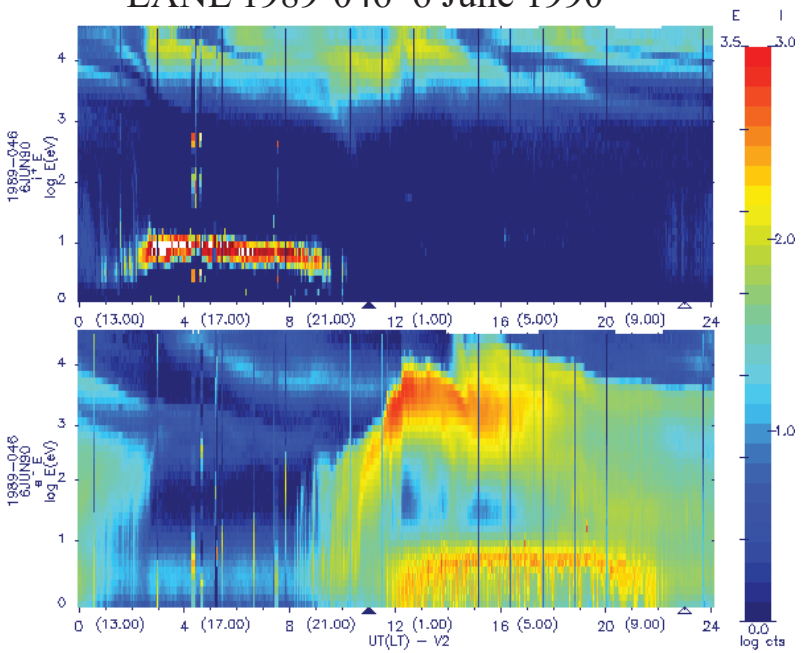
Surface charging anomalies typically occur in midnight to dawn local time sector where hot electrons are injected during geomagnetic substorms



Record ATS-6 charging event
$\Phi \sim -19$ kV

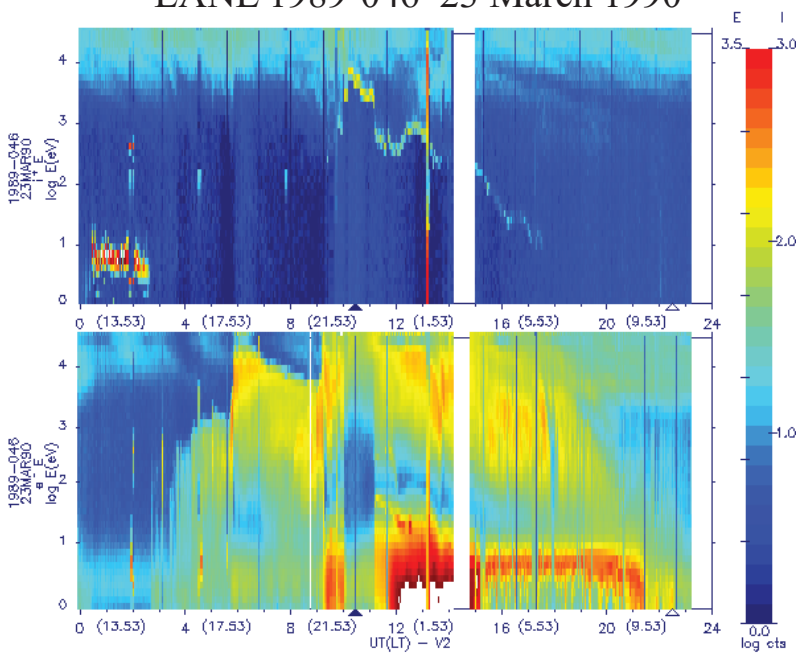
GEO Satellite Surface Charging

LANL 1989-046 6 June 1990



no charging

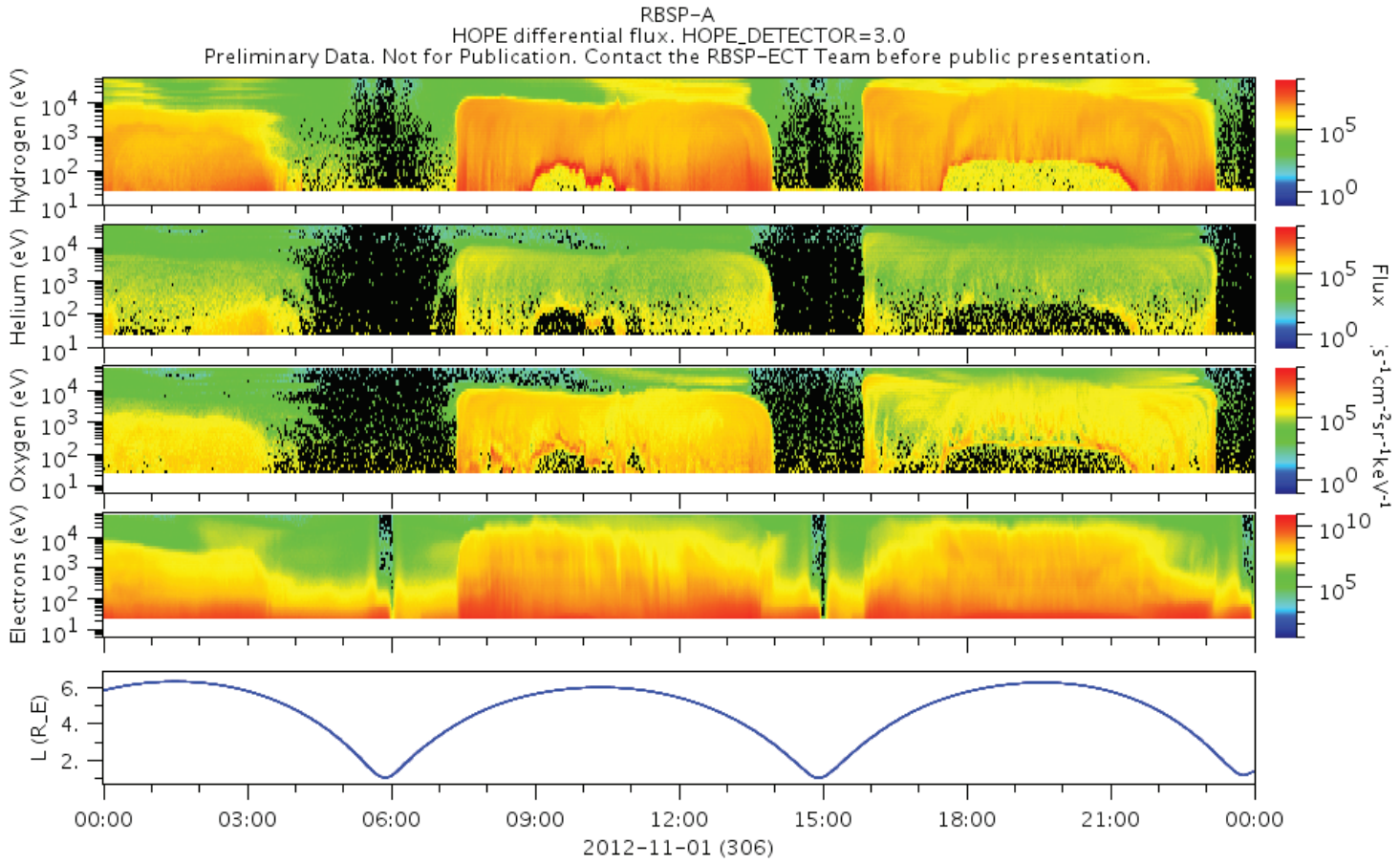
LANL 1989-046 23 March 1990



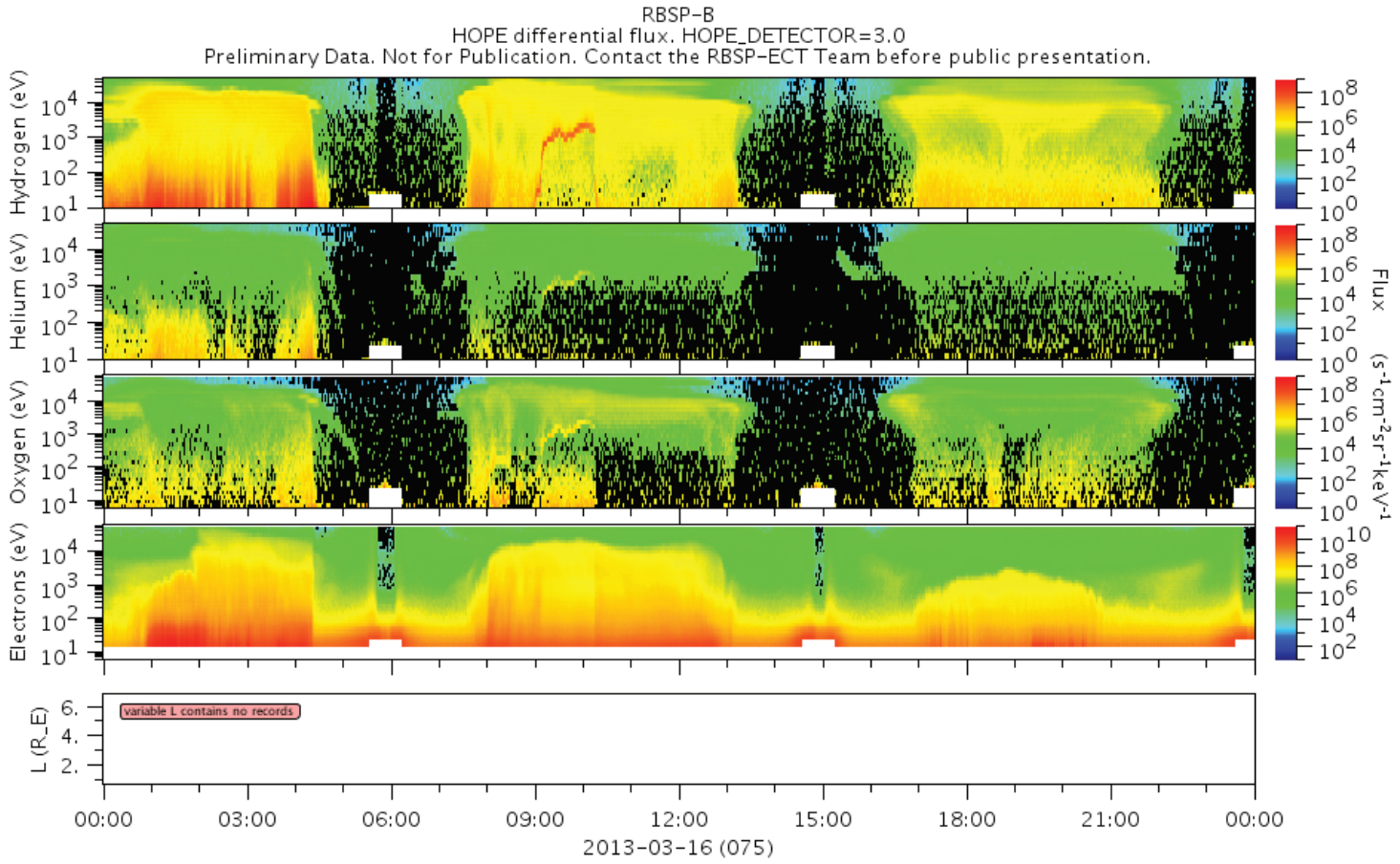
~ 8 kV in eclipse

~ 1 kV post midnight

Van Allen Probe-A: Charging to -200 V

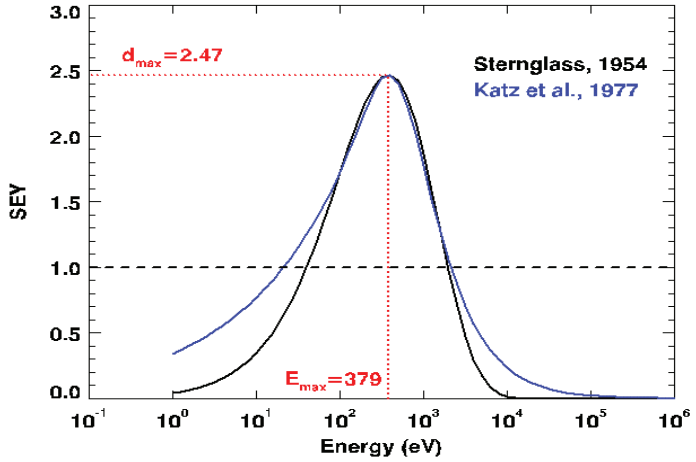


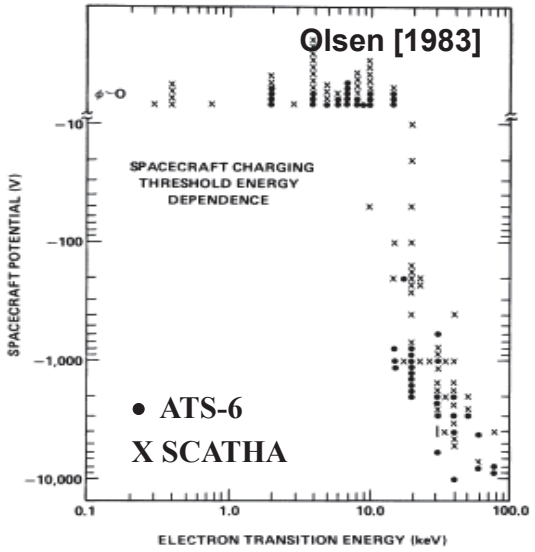
Van Allen Probe-B: Charging to -2000 V

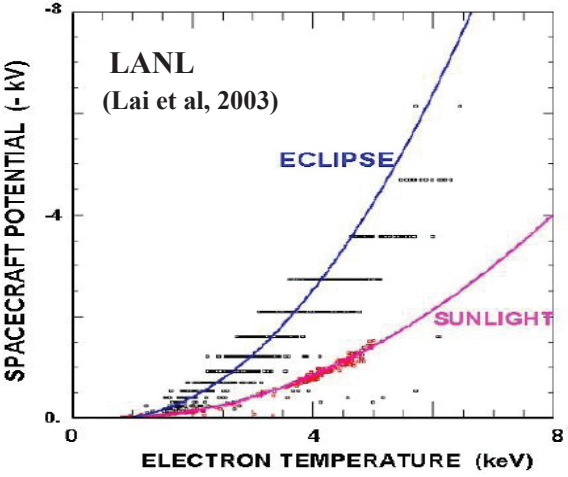


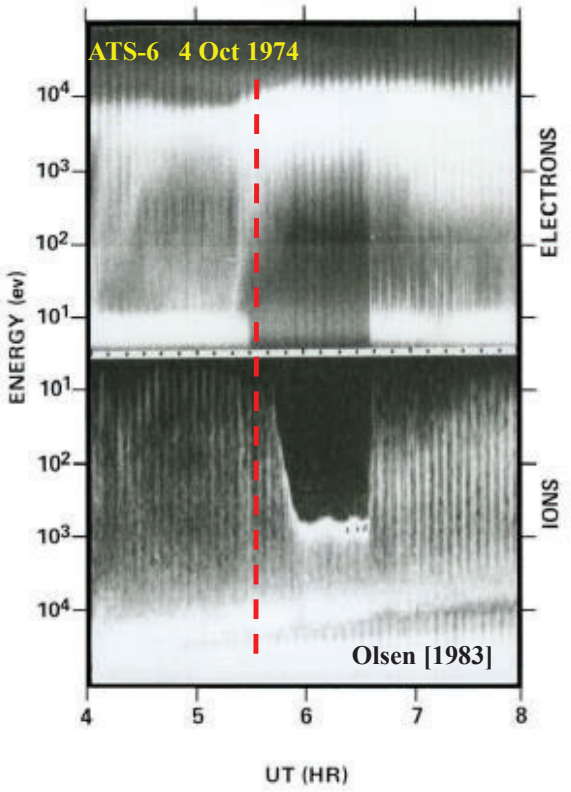
Threshold for Charging Onset

- Significant negative charging doesn't begin until enough electrons in environment have energies greater than second cross over point
- Electron energy threshold for onset of charging is due to second crossover point of secondary electron yield curves (Olsen, 1983)

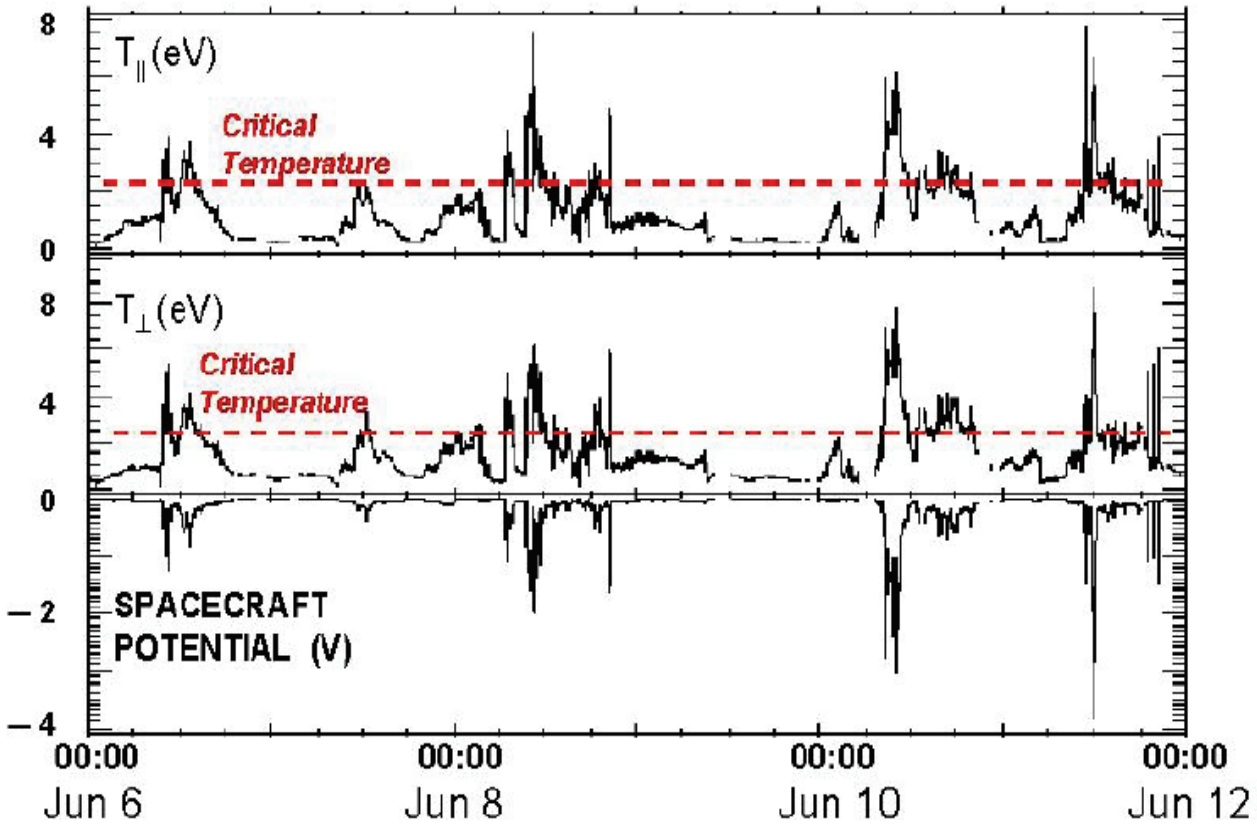








Examples of T_{crit} for Charging Onset



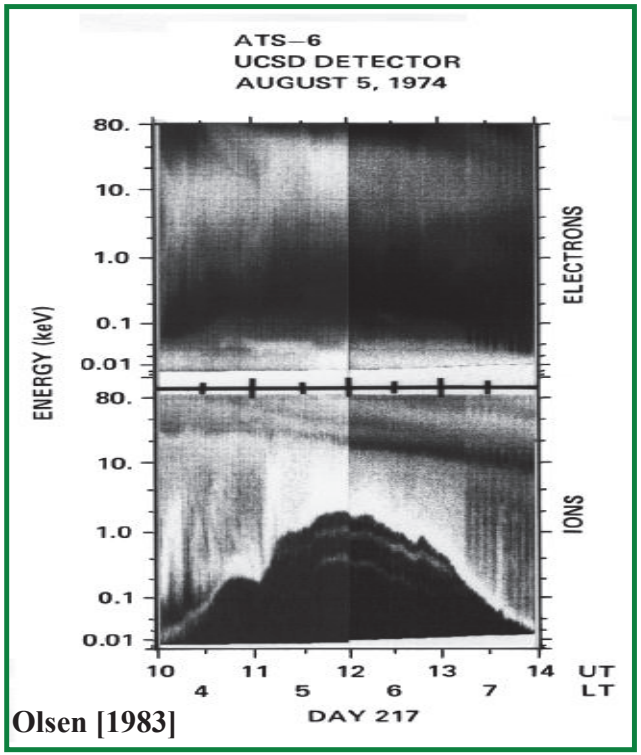
Examples of charging onset at a critical temperature, below which charging does not occur

Material	Critical Temp (keV)* Isotropic	Normal
Mg	0.4	---
Al	0.6	---
Ag	2.7	1.2
Au	4.9	2.9
Cu-Be	2.1	1.4
Al_2O_3	2.0	1.2
SiO_2	2.6	1.7
MgO_2	3.6	2.5
InO_2	3.6	2.0
MgF_2	10.9	7.8
Kapton	0.8	0.5
Teflon	2.1	1.4
Glass	2.2	1.4

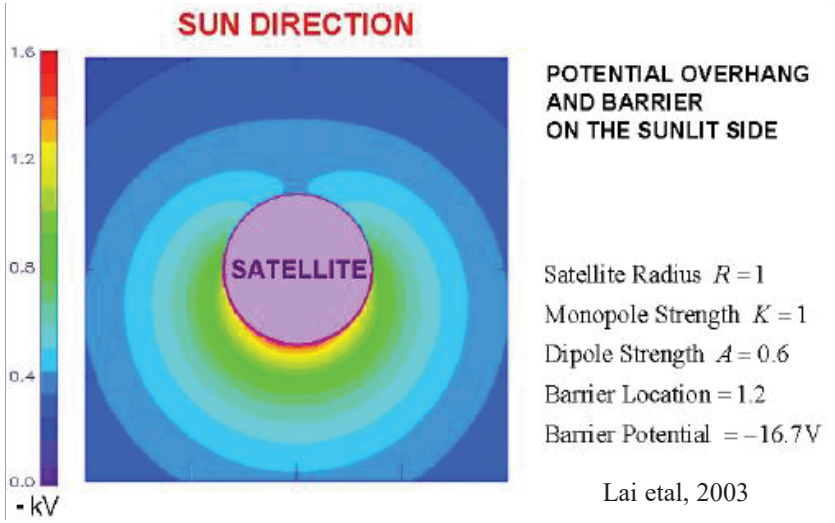
*adapted from Lai, 2008

Trapped Photoelectrons and Sunlight Charging

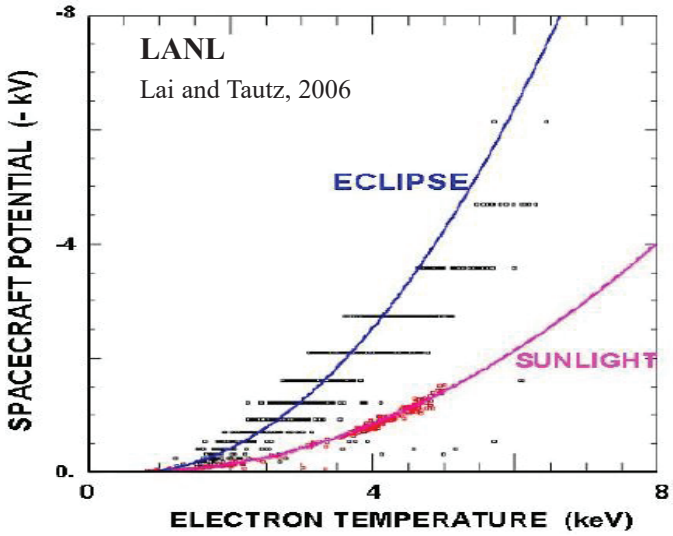
- There are cases in GEO where photoemission does not eliminate surface charging
- Dielectrics in sunlight can also charge to negative potentials



Olsen [1983]



Lai etal, 2003



Auroral Charging

- Satellites in polar orbits passing through auroral arcs may charge when the electron flux is dominated by high energy (about ≥ 10 keV) electrons

- Auroral charging is strongly controlled by
  - Energy of primary electrons and secondary electron yields
  - Density of ambient plasma (to balance auroral electron collection)

- Examples of low Earth orbit spacecraft charging in the auroral zone include
  - DMSP ~830 km, 98 deg
    -10's V > Φ > -1500 V
  - Freja 590 km x 1763 km, 63 deg
    -10's V > Φ > -3000 V



Image: M. Thiessen
National Geographic Image Collection



Image: M. Varik/greenlander

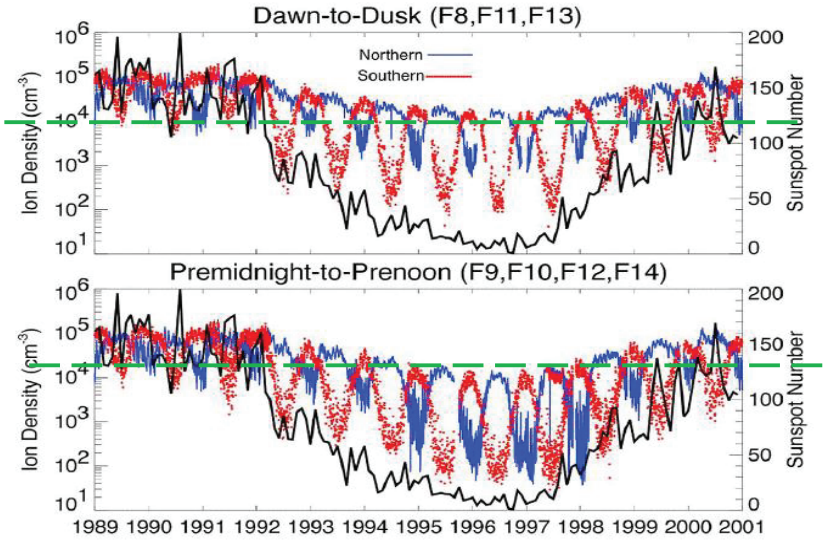
Auroral Charging and Solar Cycle

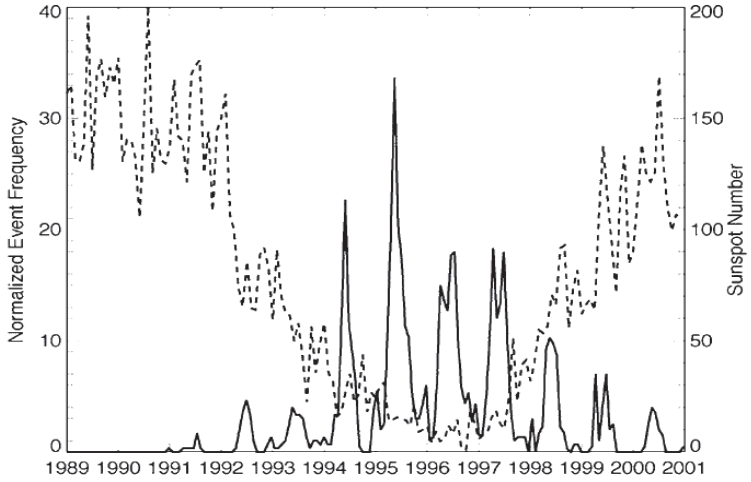
- Auroral charging studies using space environment records from the DMSP satellites have shown a strong dependence on solar cycle for occurrence of auroral charging, with charging frequency peaking during solar minimum and little or no charging during solar maximum
  - *Frooninckx and Sojka*, 1992
  - *Anderson*, 2012
  - *Meng et al*., 2019

- Necessary environmental conditions for DMSP satellites to charge when passing through the aurora [*Gussenhoven et al*, 1985]:
  - Spacecraft in darkness (no photoemission)
  - Thermal plasma density < 10^4 cm^{-3}
  - Integral number flux $J_{electrons}(\geq 10\ keV) > 10^8$ $1/cm^2\text{-}s\text{-}sr$

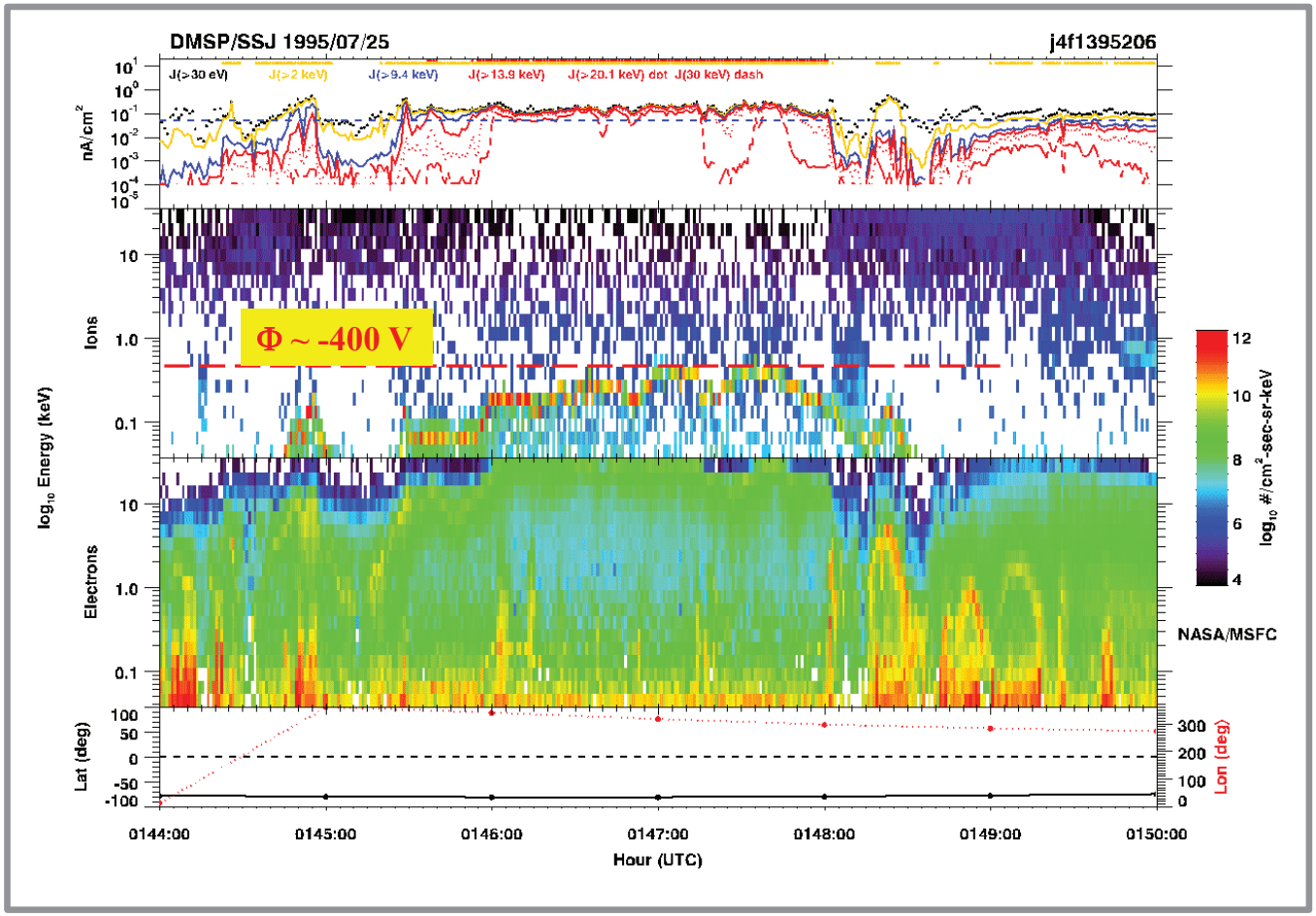
- Ambient thermal plasma suppresses charging
  - Thermal plasma is generated by photoionization of the neutral atmosphere
  - Solar UV/EUV emissions peak at solar maximum creating background plasma densities exceeding the charging density limit

- Designers for LEO polar missions might assume they can ignore charging mitigation in their spacecraft designs if they will only be operating during solar maximum conditions

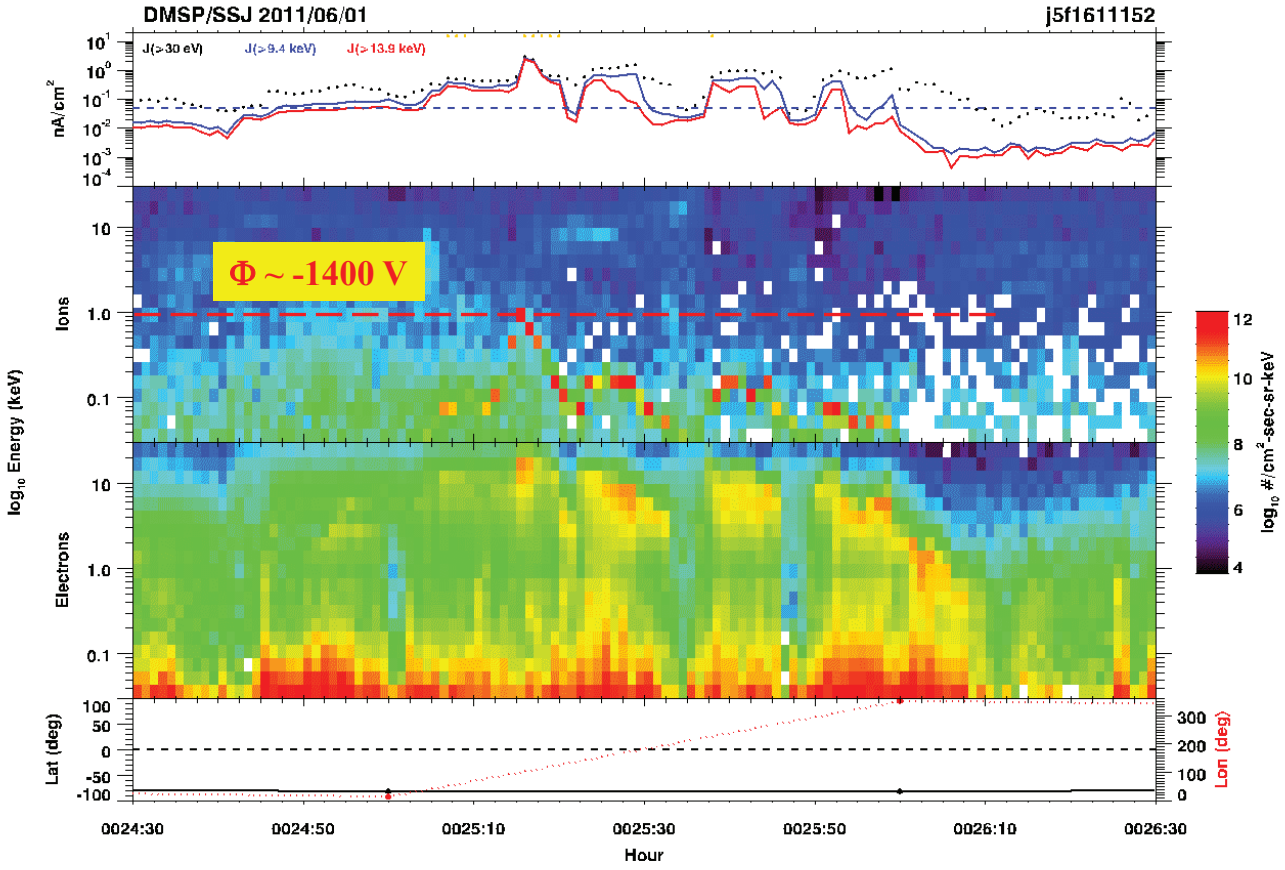




Auroral Charging Example: -400 V



Auroral Charging Example: -1,400 V



Solar Max Auroral Charging

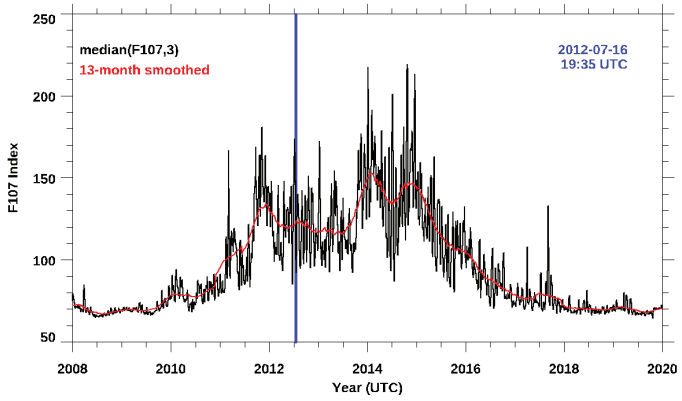
Solar Cycle 24: Solar Maximum

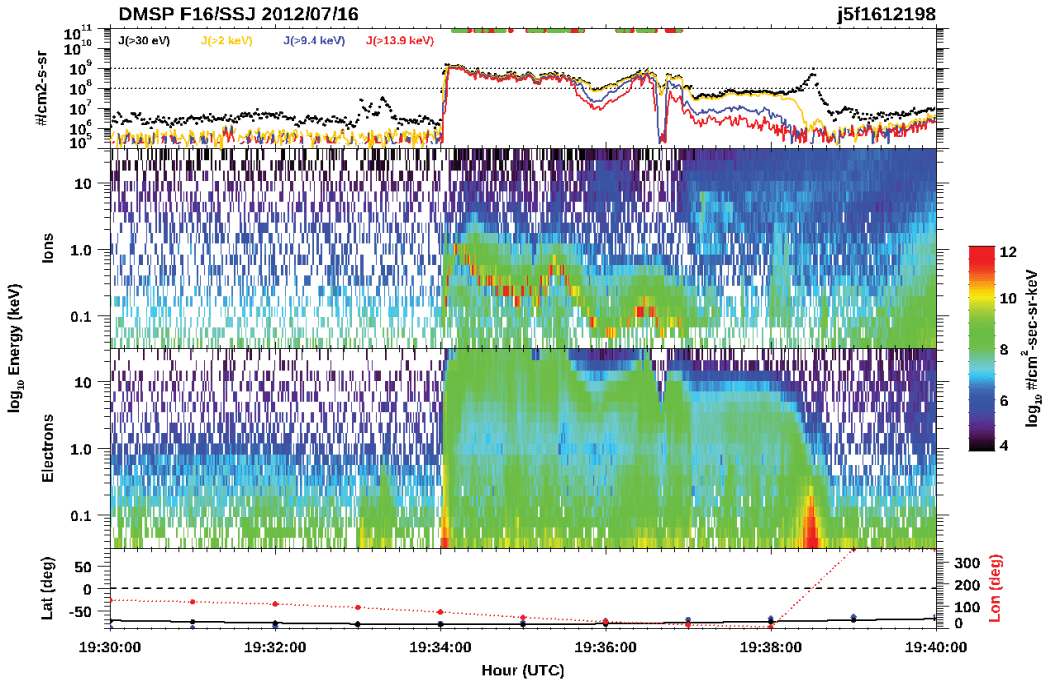
DMSP F16, 16 July 2012 19:35 UTC

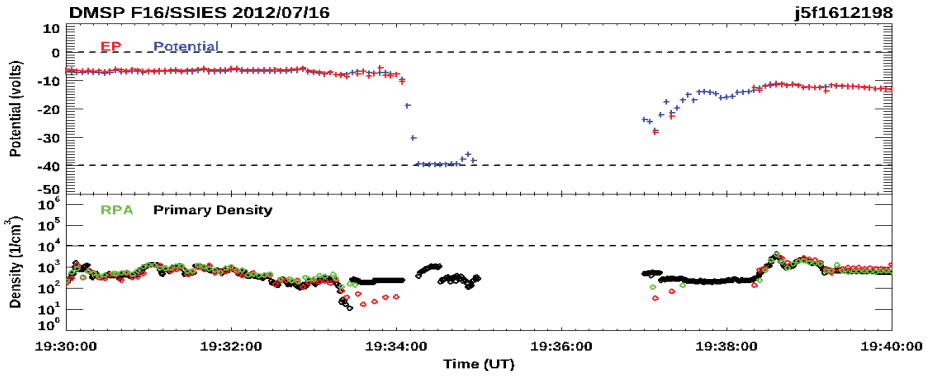
- Maximum potential: -949 V
- Average potential: -239.2 V
- Duration: 177 sec
- Southern hemisphere winter (dark)
- Plasma density ~ 10^3 cm^{-3}
- Je(>9.4 keV) ~ 10^8 to 10^9 $1/cm^2$-s-sr

Solar activity

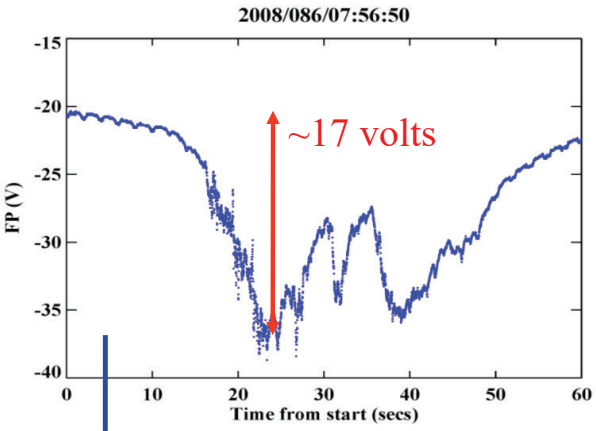
- F107 154.4 sfu
- $\langle F107 \rangle_{\text{Last 81 days}}$ 128.3 sfu

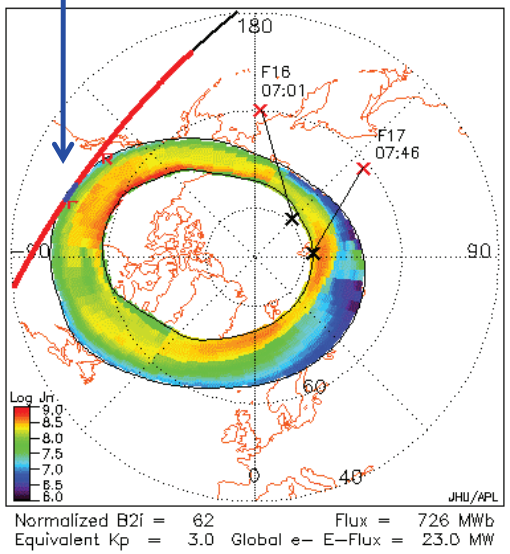


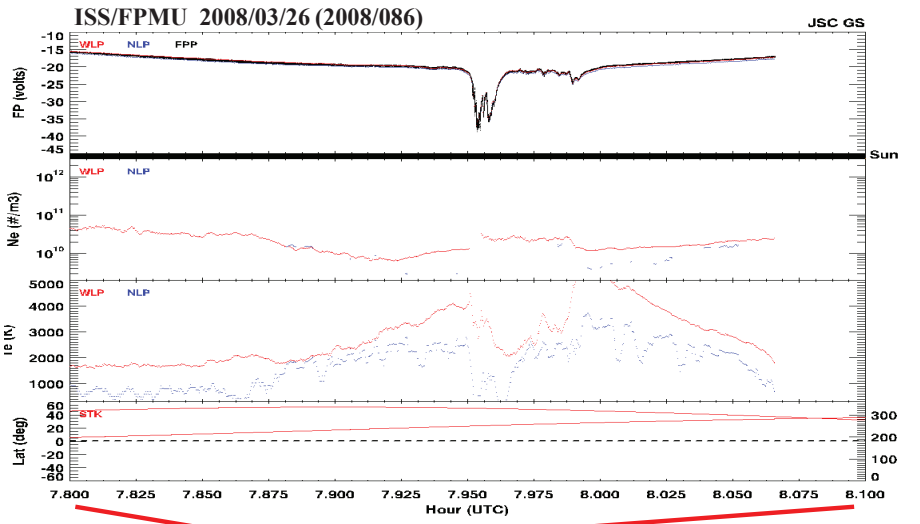


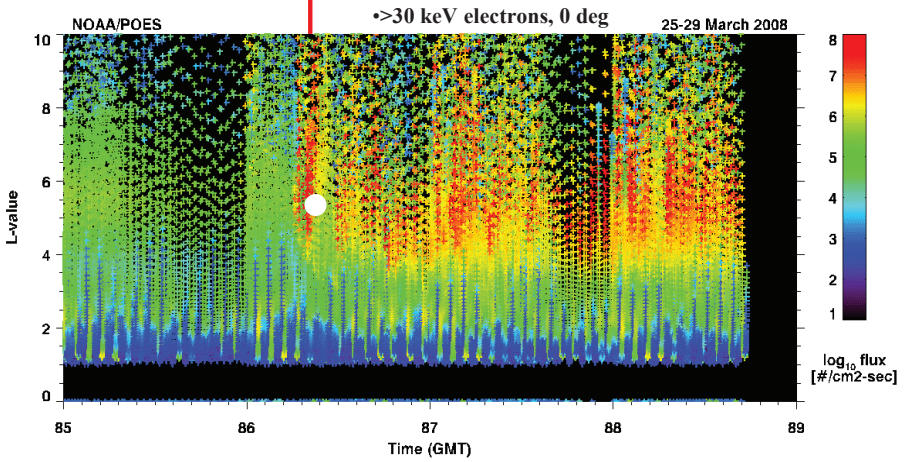


ISS Auroral Charging



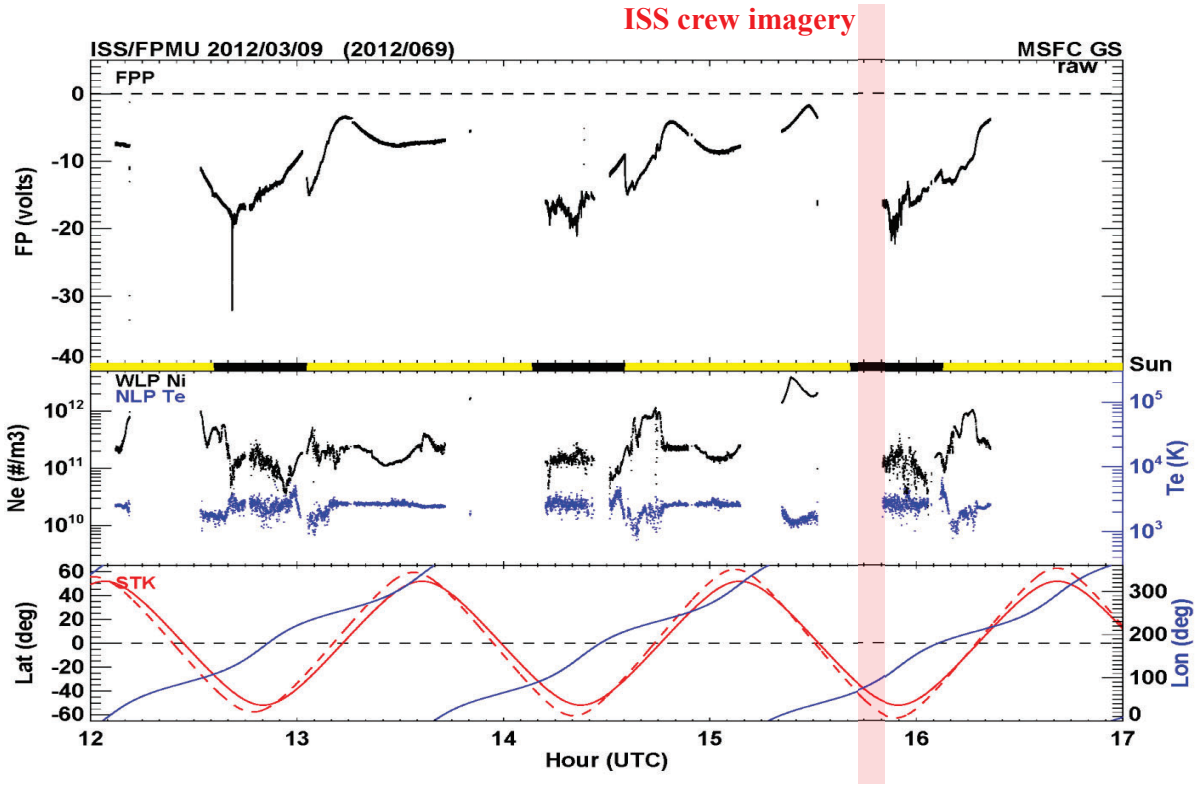






[adapted from *Craven et al.*, 2009]

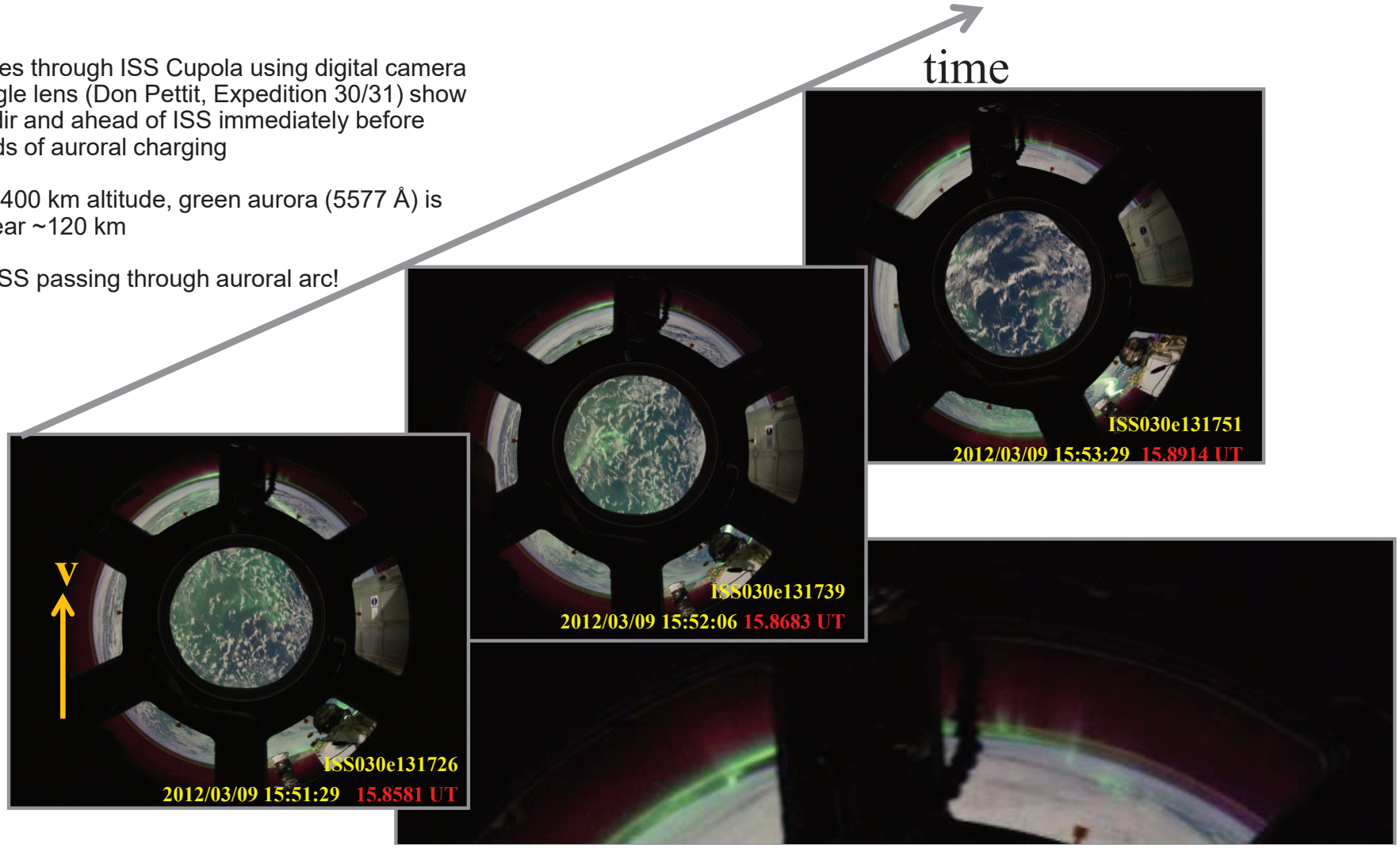
9 March 2012: FPMU



mlat - - - - - - - -

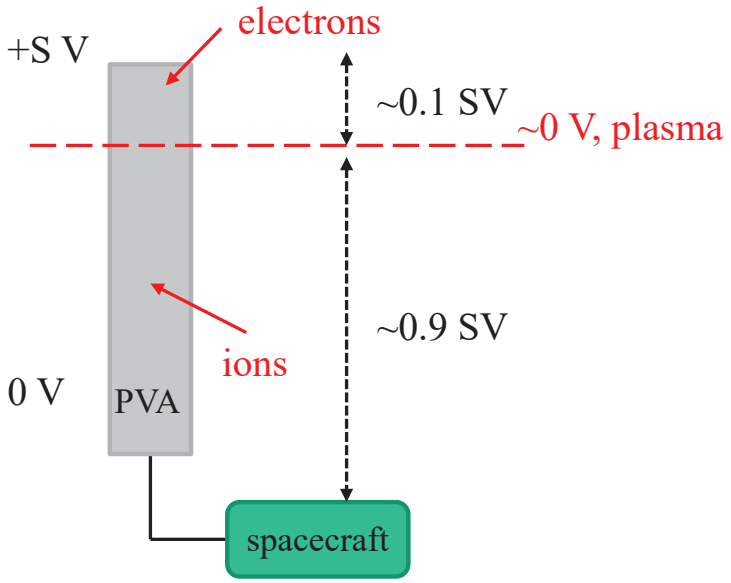
9 March 2012: Auroral Images

- Auroral images through ISS Cupola using digital camera with wide angle lens (Don Pettit, Expedition 30/31) show aurora in nadir and ahead of ISS immediately before FPMU records of auroral charging
- ISS is near ~400 km altitude, green aurora (5577 Å) is below ISS near ~120 km
- Documents ISS passing through auroral arc!



Photovoltaic Array Interaction with Plasma Environment

- **Spacecraft with photovoltaic array (PVA) grounded to vehicle on negative end of array can exhibit negative charging to ~90% of the array string voltage**
  - Minor issue for low ~30 V string voltages that are widely used on US spacecraft
  - Can be an issue for high voltage systems with string voltages of 100's V or more
  - Probability for arcing increases dramatically in LEO when the string voltage exceeds ~200 V



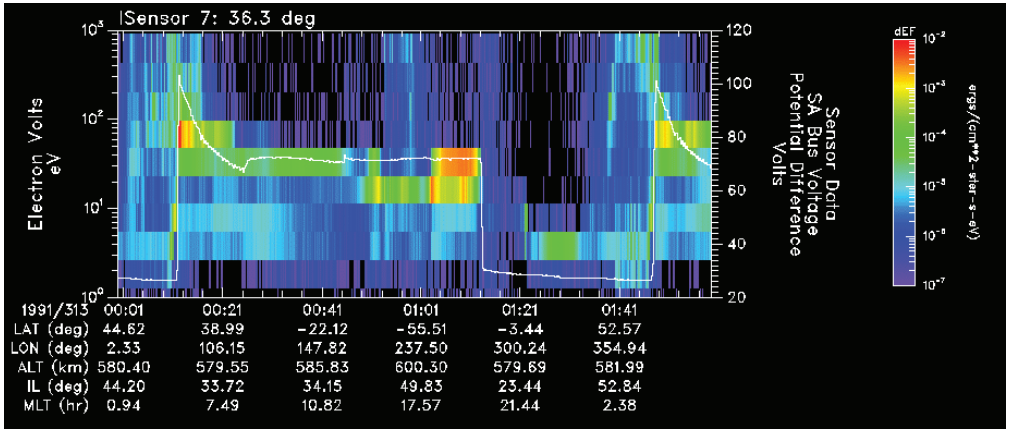
Photovoltaic Array Interaction with Plasma Environment

- **Spacecraft with photovoltaic array (PVA) grounded to vehicle on negative end of array can exhibit negative charging to ~90% of the array string voltage**
  - Minor issue for low ~30 V string voltages that are widely used on US spacecraft
  - Can be an issue for high voltage systems with string voltages of 100's V or more
  - Probability for arcing increases dramatically in LEO when the string voltage exceeds ~200 V

- **Upper Atmospheric Research Satellite (UARS)**
  - NASA, Southwest Research Institute
  - 09/1991 – 09/2005 (decommissioned)
  - Orbit: 574 km x 575 km x 57° inc
  - PVA voltage varies from 100 V (cold) to 75 V (warm)
  - Charging at eclipse exit to ~ -90 V



Image: NASA



UARS solar array voltage and satellite frame potential (Frahm, 2000; Carruth and Vaughn, 2000)

Photovoltaic Array Interaction with Plasma Environment

- **Spacecraft with photovoltaic array (PVA) grounded to vehicle on negative end of array can exhibit negative charging to ~90% of the array string voltage**
  - Minor issue for low ~30 V string voltages that are widely used on US spacecraft
  - Can be an issue for high voltage systems with string voltages of 100's V or more
  - Probability for arcing increases dramatically in LEO when the string voltage exceeds ~200 V

- **HORYU-II**
  - JAXA, Kyushu Institute of Technology
  - 05/2012 – operational?
  - Orbit: 651 km x 671 km x 98.2° inc
  - High voltage test PVA to 350 V
  - Charging at eclipse exit observed to over -300 V

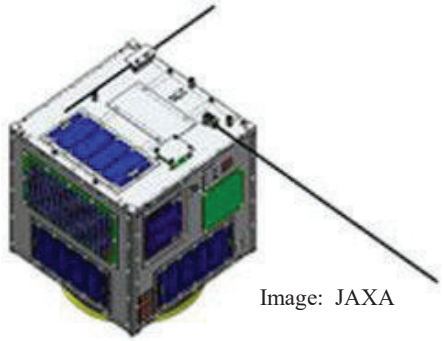


Image: JAXA

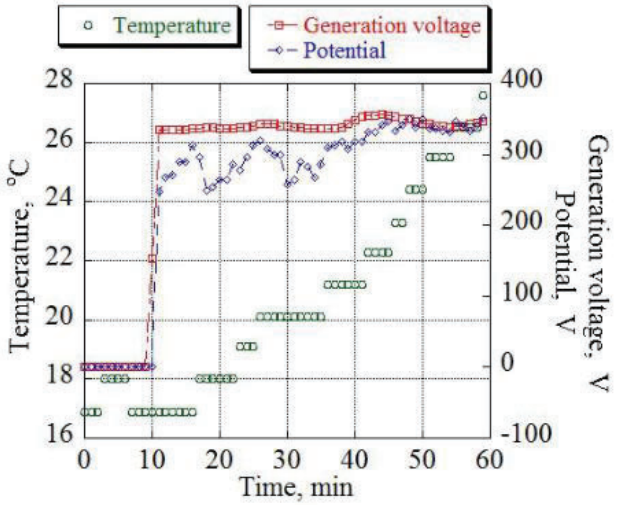
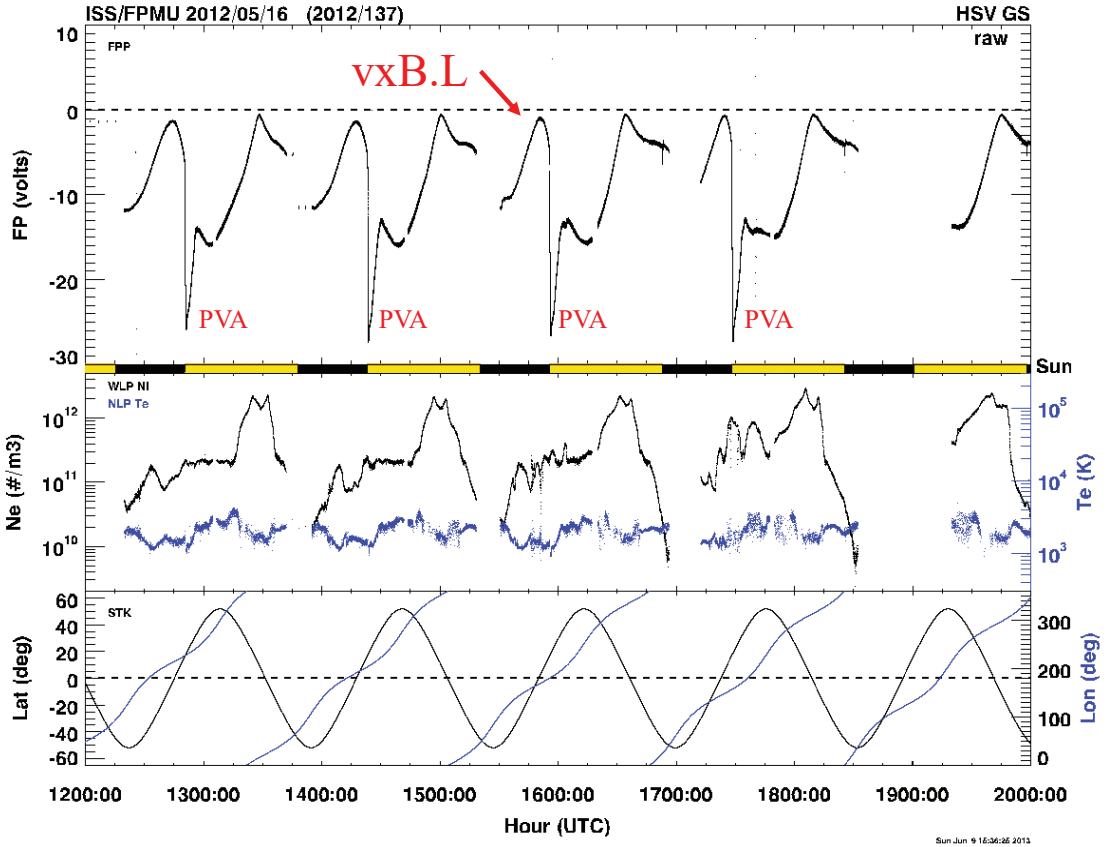


Figure 5: Result of 300V generation

(Seri et al., 2013; Cho et al., 2014)

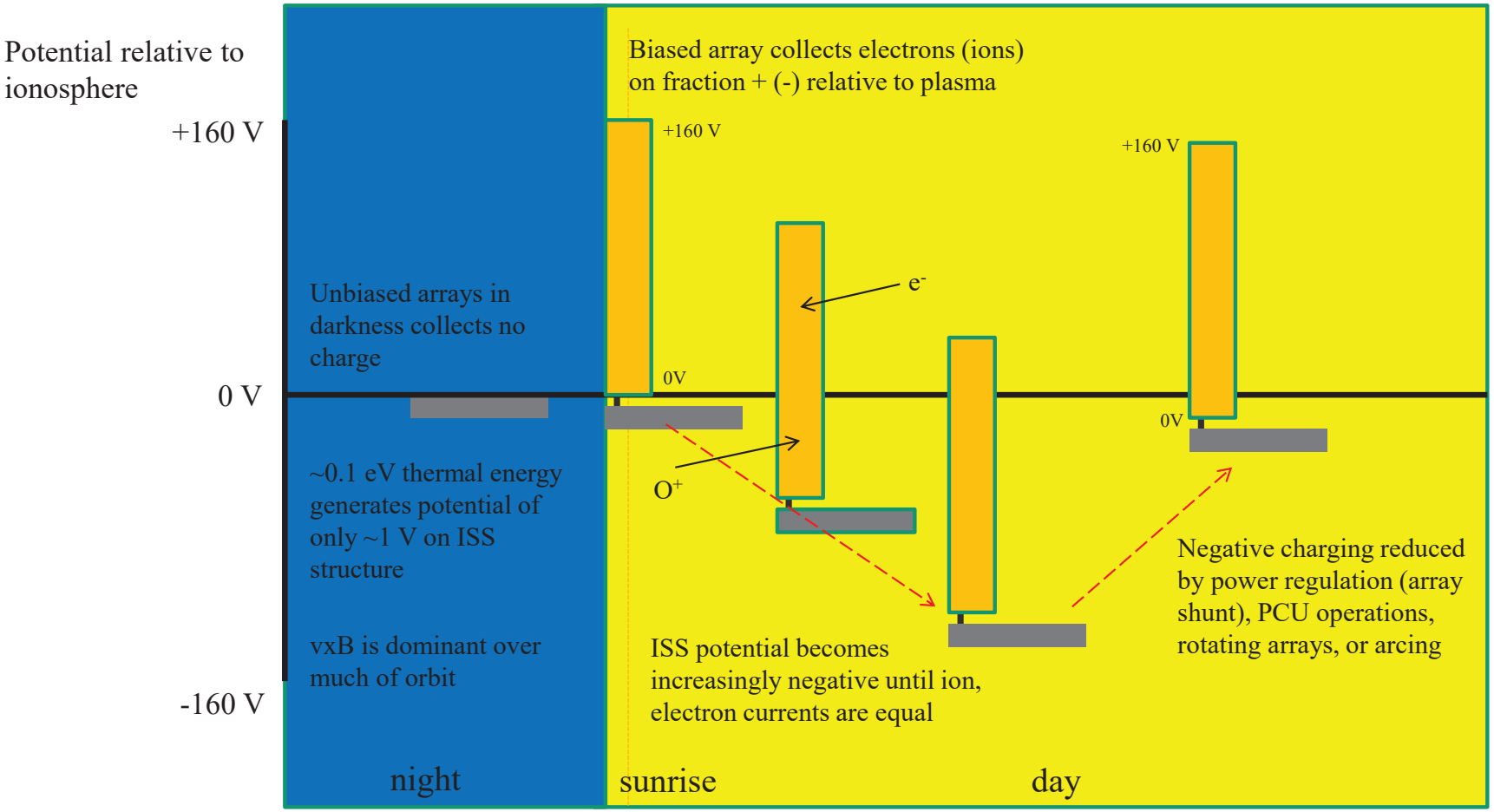
ISS Potential Variations

- ISS potential variations are due to
  - Current collection by US 160 V photovoltaic arrays (PVA)
  - Inductive (vxB).L across structure
  - Auroral charging
  - Visiting vehicles with high voltage PVAs
  - Payloads with current sources
- ISS structure is generally negative with respect to plasma since PVAs are grounded to structure on the negative end of the arrays
- Charging peaks following eclipse exit when arrays are biased, current collecting surfaces are in ram, and batteries are charging
- Charging decreases over daylight segment of orbit as strings are shunted when power needs decrease and arrays tracking the Sun rotate into wake



(Minow et al. 2022)

ISS Solar Array Charging



+160 V

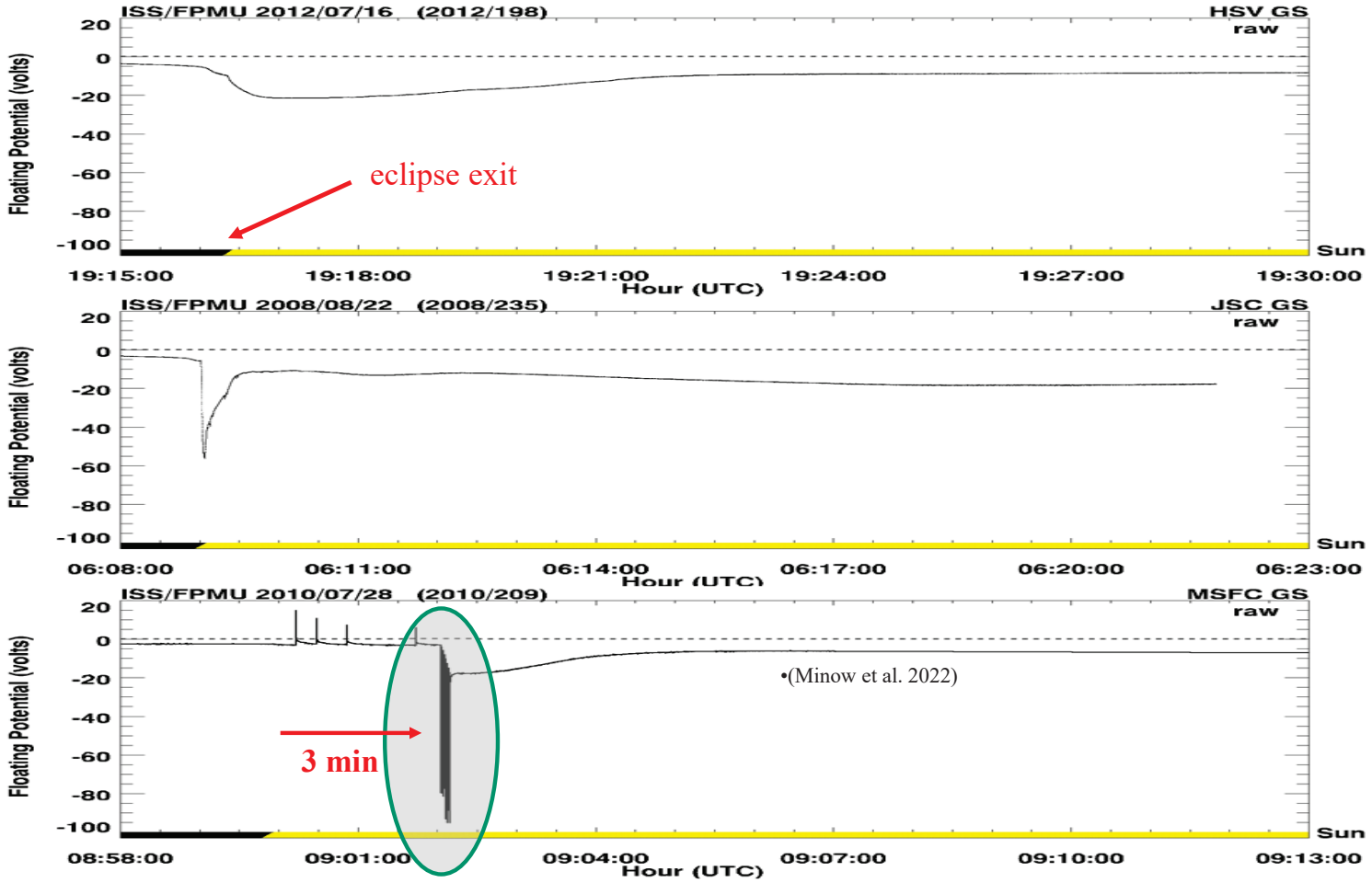
0V

PVA Negative Charging

Normal Charging

Rapid Charging Event (RCE)

Sunlight Unshunt

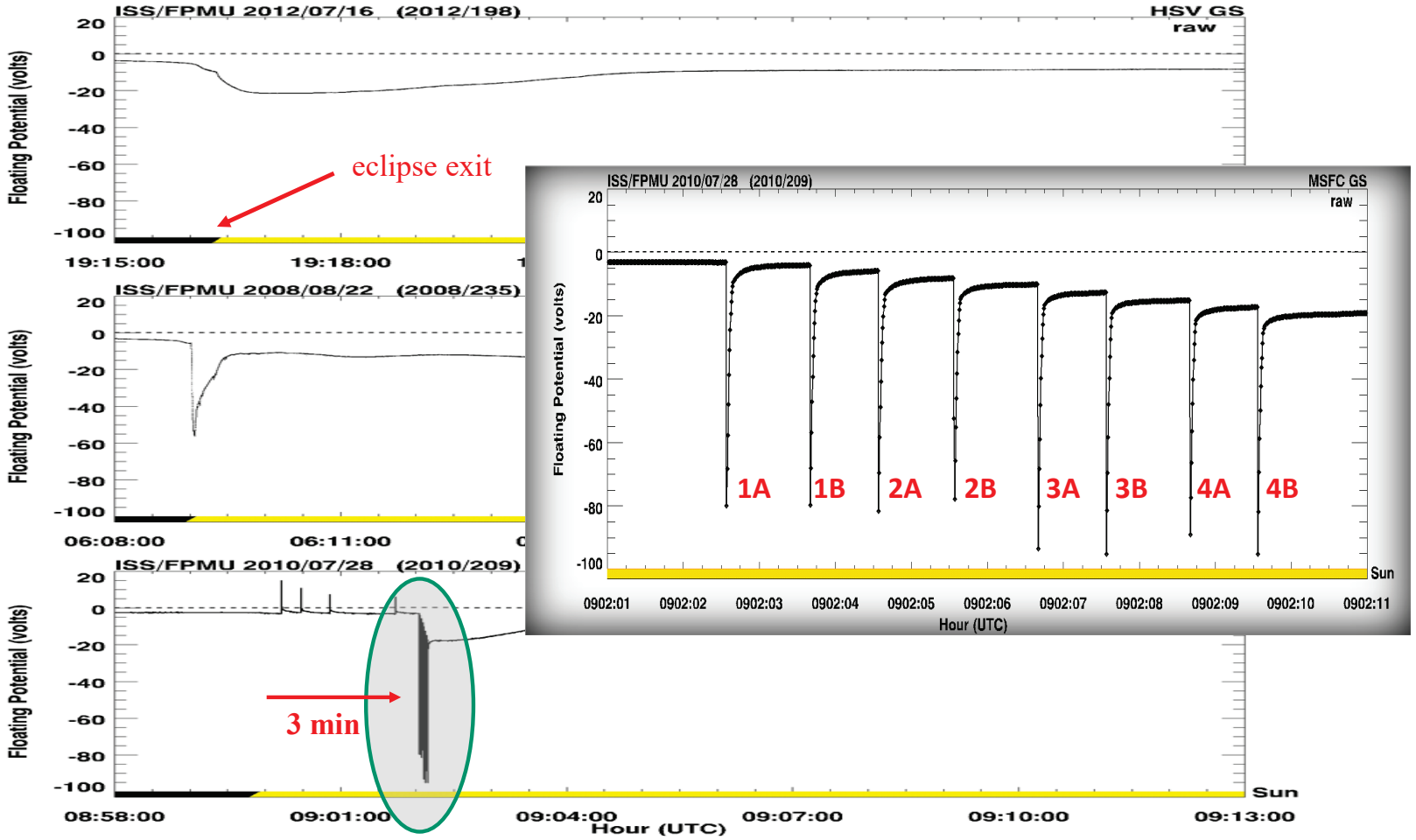


PVA Negative Charging – 2010 Sunlight Unshunt Experiment

Normal Charging

Rapid Charging Event (RCE)

Sunlight Unshunt



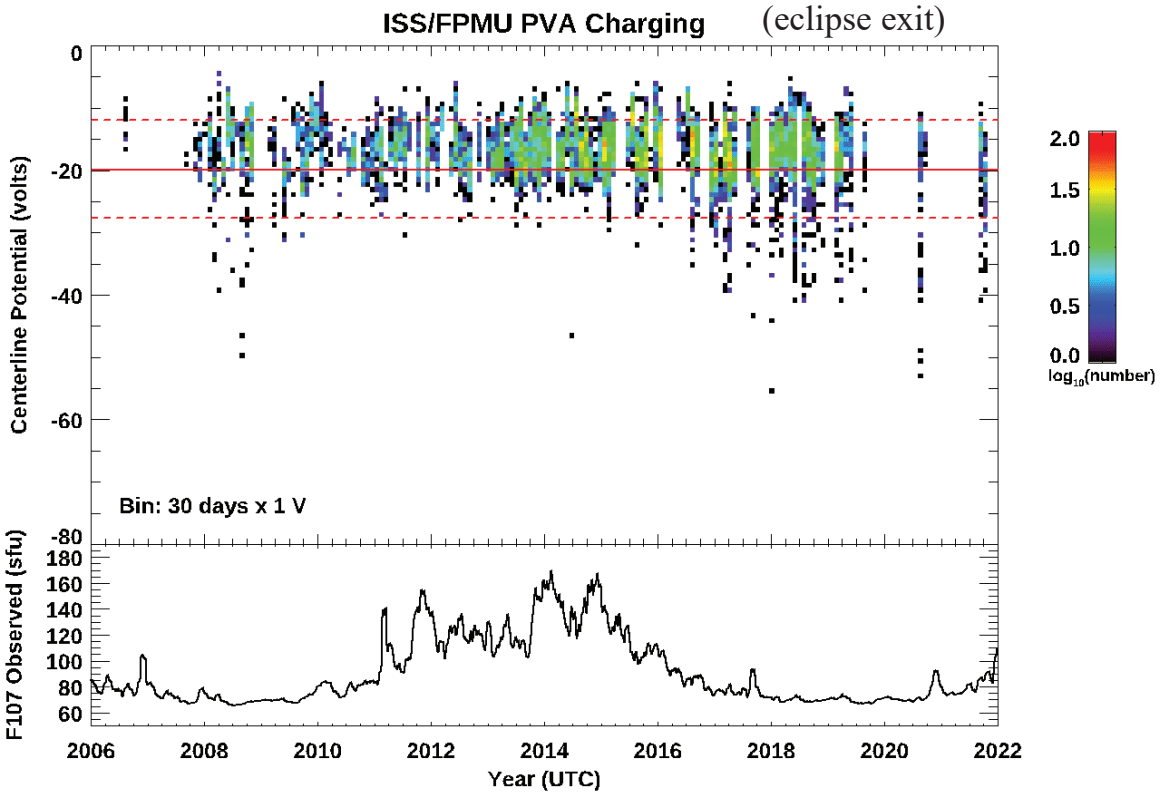
(Minow et al. 2022)

ISS PVA Charging Statistics and Solar Cycle

- PVA normal negative charging typically peaks in the range of -10 V to -30 V:

5%	-12.0 V
50%	-19.9 V
95%	-27.6 V

- Largest PVA RCE negative charging in the -35 V to -70 V range occurs at eclipse exits with low plasma densities
- RCEs correlate with solar cycle (because the low plasma density events are a function of solar activity)
- Largest ISS charging events observed to date are in the range of -90 V to -100 V and occur during PVA unshunt operations in full sunlight



Geotail: Photoelectron Charging

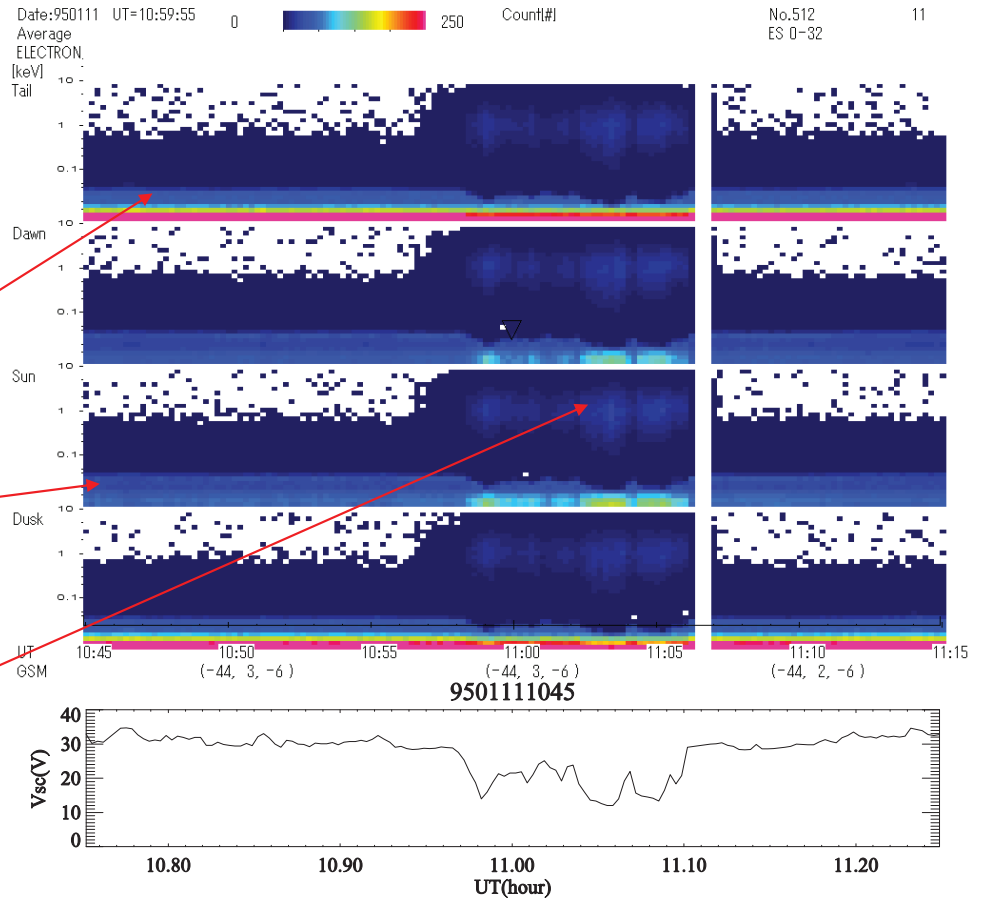
- Photoelectron currents can dominate the charging process in low density environments, spacecraft charges positive to some 10's volts
- In this example, the Geotail spacecraft is in magnetotail where

$$J_{ph} > J_{plasma}$$

spacecraft photoelectrons with energy >+qΦs/c escape, lower energy photoelectrons are trapped

plasma sheet Te ~ 100's eV

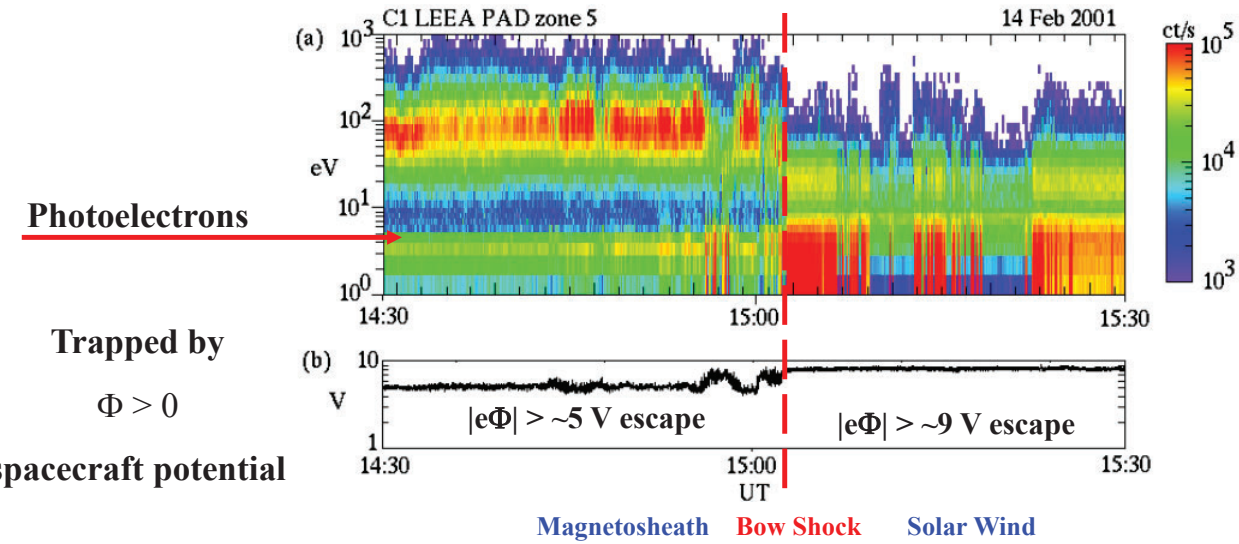
Increase hot electron flux reduces positive spacecraft charge and lower energy photoelectrons can escape



Shimoda et al., 9th SCTC

Magnetosheath, Solar Wind

- Cluster spacecraft outbound from magnetosheath into solar wind
- High density magnetosheath plasma provides some current to balance photoelectron current, reducing positive potential but net potential is still positive
- Low density solar wind environment cannot balance photoelectrons and spacecraft positive potential increases



(from Szita et al., 2001)

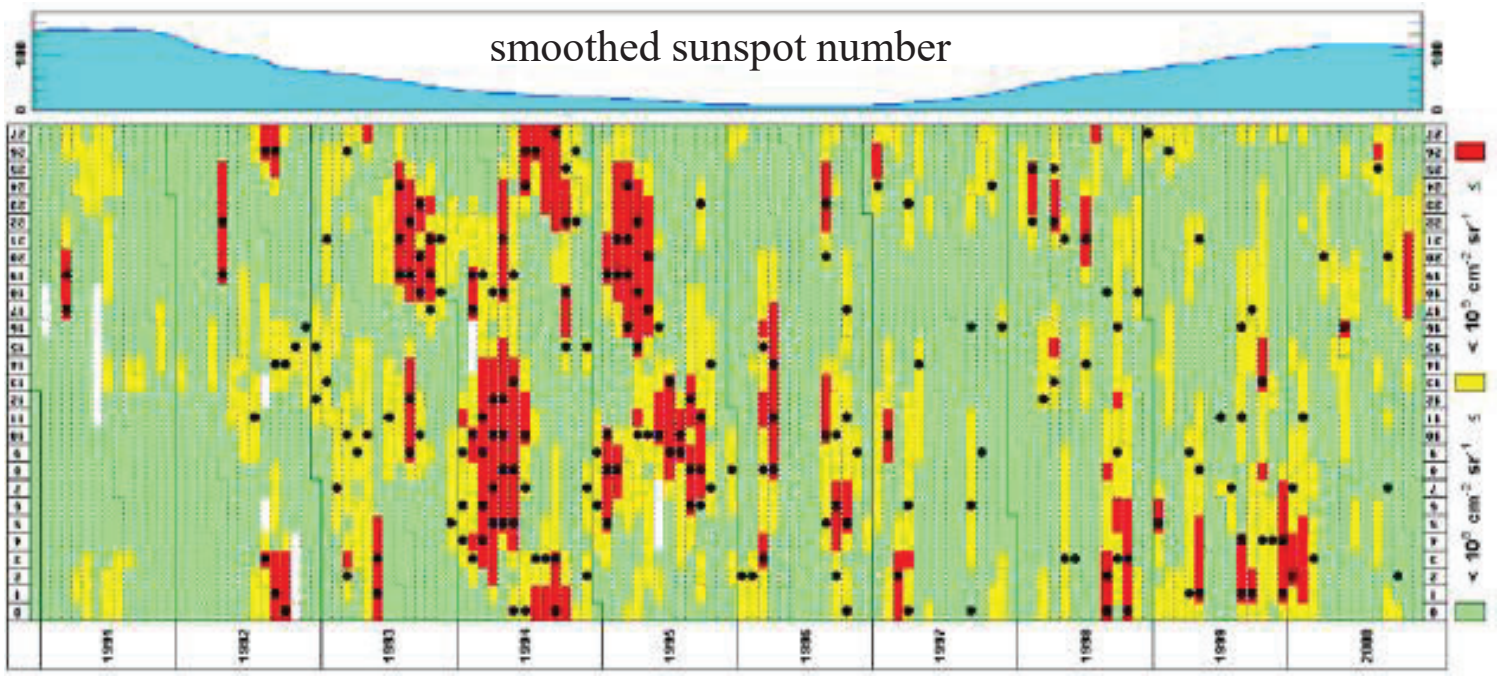
Internal (Deep Dielectric) Charging

- High energy (>100 keV) electrons penetrate spacecraft walls and accumulate in dielectrics or isolated conductors
- Threat environment is energetic electrons with sufficient flux to charge circuit boards, cable insulation, and ungrounded metal faster than charge can dissipate
- Accumulating charge density generates electric fields in excess of breakdown strength resulting in electrostatic discharge
- System impact is material damage, discharge currents inside of spacecraft Faraday cage on or near critical circuitry, and RF noise



PMMA (acrylic) charged by ~2 to 5 MeV electrons

GOES Solar Cycle 21 Internal Charging Anomalies (GEO)



Black: GOES phantom commands [*Wrenn et al.* 2002]

2-day fluence (F2) > 2 MeV electrons

Red: F2 $\geq 10^9$ e$^-$/cm^2-sr

Amber: 10^9 > F2 $\geq 10^8$ e$^-$/cm^2-sr

Green: F2 < 10^8 e$^-$/cm^2-sr

White: no data

Internal Charging: Physics

$$\nabla \bullet \varepsilon E = \rho$$ Poisson equation

$$\varepsilon = \kappa \varepsilon_0$$ permittivity

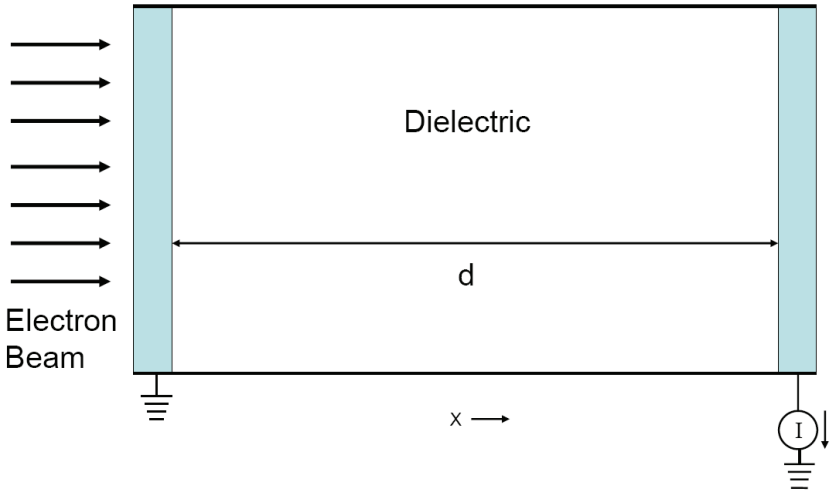
$$\frac{\partial \rho}{\partial t} = -\nabla \bullet J$$ Continuity equation

$$J = J_R + J_C$$ Radiation (charging) current, conductive currents

$$J_C = \sigma E$$

$$= \left[\sigma_{dark} + \sigma_{RIC}\right] E$$ Dark conductivity, radiation induced conductively

$$\sigma_{RIC} = k\left(\frac{d\gamma}{dt}\right)^{\alpha} \quad 0.5 < \alpha < 1.0$$ Radiation induced conductivity



[*Jun et al.* 2007]

Solution to Poisson, continuity equation involves two problems:

- Radiation (electron) penetration with charge and energy deposition in material
- Electrostatic solution of fields from charge distribution in insulator

Internal Charging: Electrostatic Models

Generation-Recombination (GR) Model

- Microscopic model explicitly treats the radiation generated charge carrier pairs, field induced drift of carriers, and loss through recombination
- Many parameters, difficult to obtain these for many materials

$$\epsilon \frac{\partial E}{\partial x} = \rho_+ - \rho_- - \rho_{t-} \quad (4)$$

$$\frac{\partial(\rho_- + \rho_{t-})}{\partial t} = -\frac{\partial J_0}{\partial x} + G - \alpha_f \rho_+ \rho_- - \alpha_t \rho_+ \rho_{t-} + \frac{\partial(\mu_- \rho_- E)}{\partial x} \quad (5)$$

$$\frac{\partial \rho_+}{\partial t} = G - \alpha_f \rho_+ \rho_- - \alpha_t \rho_+ \rho_{t-} - \frac{\partial(\mu_+ \rho_+ E)}{\partial x} \quad (6)$$

$$\frac{\partial \rho_{t-}}{\partial t} = \frac{\rho_-}{\tau_-}\left(1 - \frac{\rho_{t-}}{\rho_m}\right) - \alpha_t \rho_+ \rho_{t-} \quad (7)$$

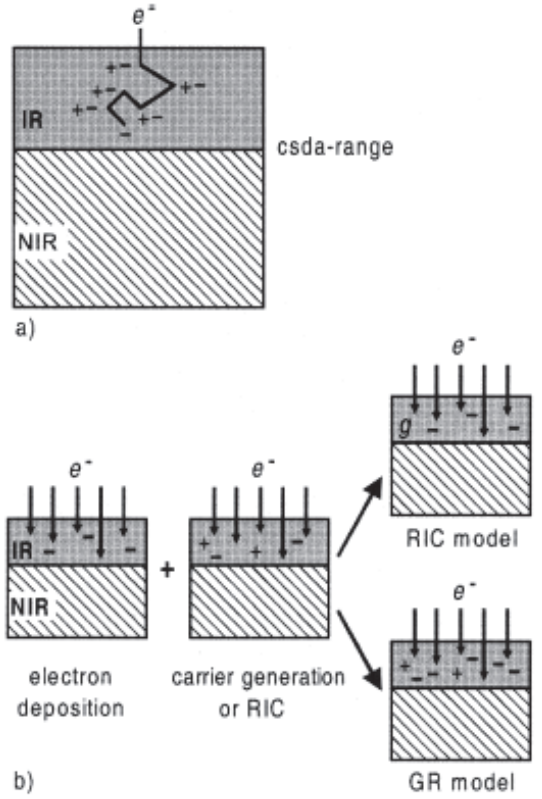
Radiation Induced Conductivity (RIC) Model

- Macroscopic model based on empirical relation ship between radiation dose and conductivity
- Less parameters, approach most used in engineering applications

$$\epsilon \frac{\partial E}{\partial x} = -\rho_- - \rho_{t-} \quad (1)$$

$$\frac{\partial(\rho_- + \rho_{t-})}{\partial t} = -\frac{\partial J_0}{\partial x} + \frac{\partial(\mu_- \rho_- E)}{\partial x} + \frac{\partial(gE)}{\partial x} \quad (2)$$

$$\frac{\partial \rho_{t-}}{\partial t} = \frac{\rho_-}{\tau_-}\left(1 - \frac{\rho_{t-}}{\rho_m}\right) \quad (3)$$



[*Sessler et al.* 2004]

DICTAT Internal Charging Code

- DICTAT model evaluates possibility of dielectric breakdown of insulating materials due to radiation charging

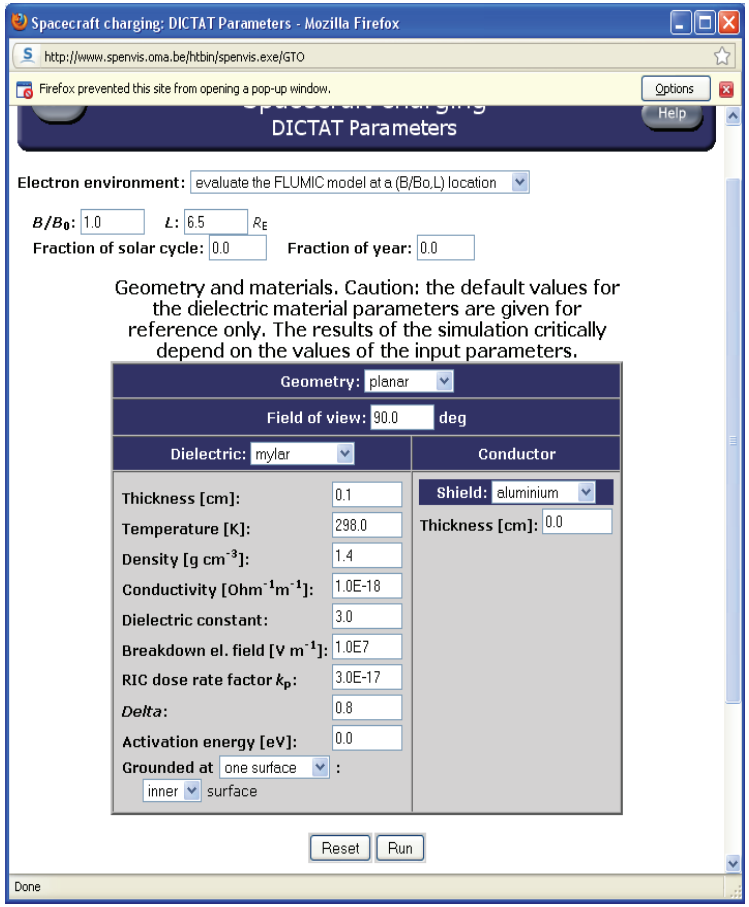
- Single material parameterized by electrical conductivity (dark and radiation induced) dielectric constant, density, temperature

  - **Example: 1 mm Mylar exposed to ESA FLUMIC (worst case) GEO electron environment**

  - **Resistivity 10^{14} Ω-m**
    After 48.0 hours: Charging current= 7.0535E-13 Amps/cm^2
    E-max= 6.5170E+05 V/m Voltage= 464.5 volts
    The dielectric IS NOT liable to experience breakdown
    Maximum E lower than Breakdown field= 1.00E+07 V/m

  - **Resistivity 10^{16} Ω-m**
    After 48.0 hours: Charging current= 7.0535E-13 Amps/cm^2
    E-max= 1.4130E+07 V/m Voltage= 1.1678E+04 volts
    The dielectric IS liable to experience breakdown
    Maximum E higher than Breakdown field= 1.00E+07 V/m

  - **Resistivity 10^{18} Ω-m**
    After 48.0 hours: Charging current= 7.0535E-13 Amps/cm^2
    E-max= 3.5881E+07 V/m Voltage= 2.8170E+04 volts
    The dielectric IS liable to experience breakdown
    Maximum E higher than Breakdown field= 1.00E+07 V/m



http://www.spenvis.oma.be/

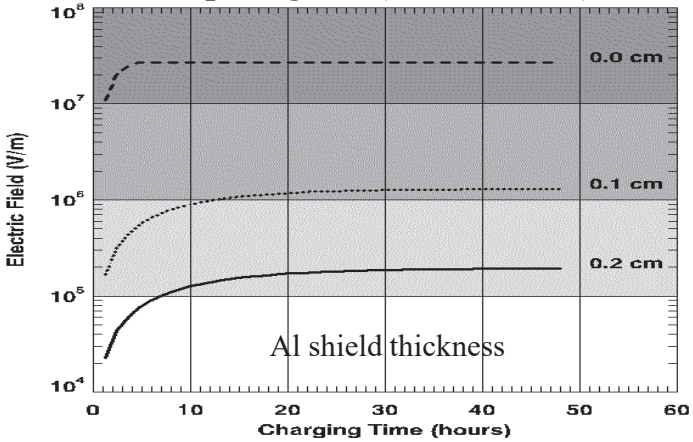
DICTAT Internal Charging Analysis

- Simple first order charging evaluation along trajectories through Earth's radiation belts using standard trapped radiation models, mitigation of charging by shielding

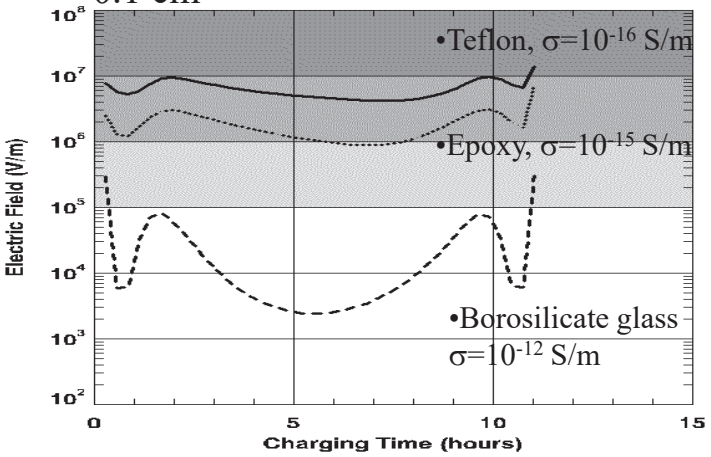
- Two example trade studies"
  - Case 1 (top):
    - 10 mm thick plexiglass shielded by aluminum 0.0 cm, 0.1 cm, and 0.2 cm thick
    - Peak AE-8 GEO radiation flux (constant)
  - Case 2 (bottom):
    - Three 0.1 cm thick materials with volume conductivity of 10^{-16}, 10^{-15}, and 10^{-12} S/m
    - AE-8 solar max electron flux
    - 250 km x 38,226 km x 0° inc, single orbit

- Grey levels indicate relative threat levels for electrostatic discharge assuming materials typically suffer dielectric breakdown at electric fields in the range of 10^6 V/m to 10^7 V/m.

10 cm plexiglass ($\sigma=10^{-15}$ S/m)

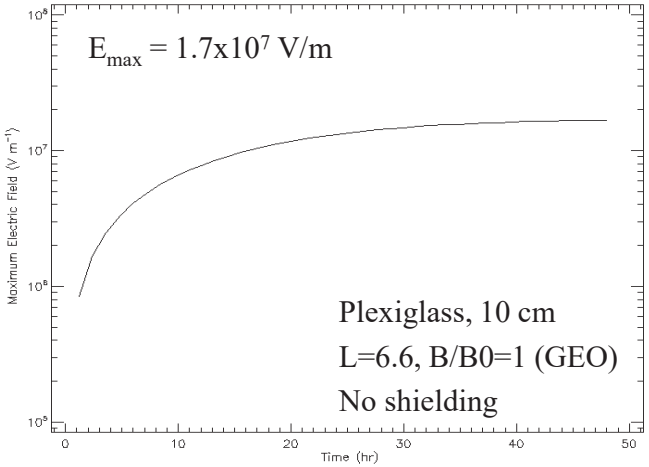


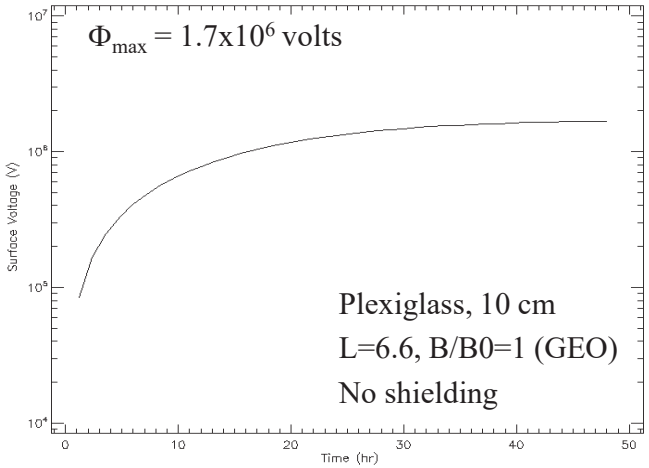
0.1 cm



DICTAT Internal Charging Analysis

- Electric field, surface voltage potential as function of time
- Allows quick screening for materials issues
- Simulation options limited by tool
  - Maximum time (48 hours)
  - Single material
  - Constant flux for user input
  - Radiation belt models for time variations in radiation flux
  - Only maximum E field is reported, no information on electric field as function of depth



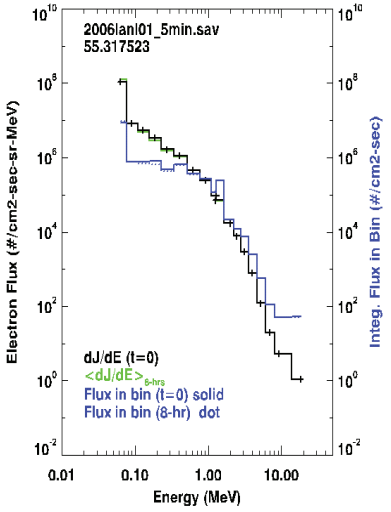


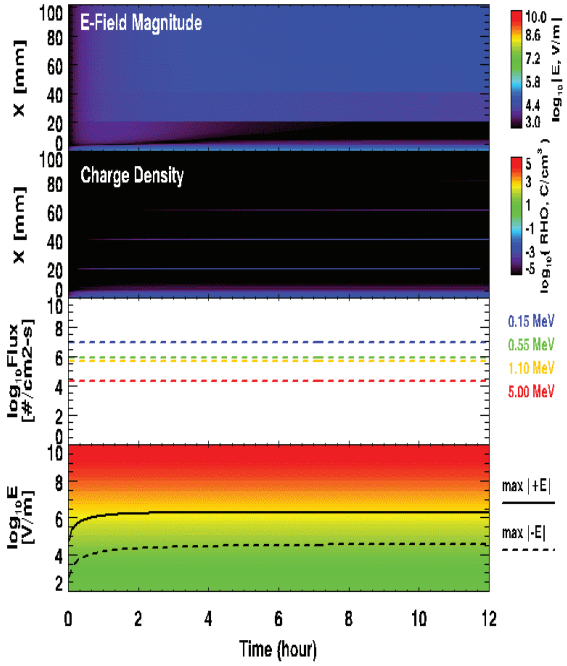
http://www.spenvis.oma.be/

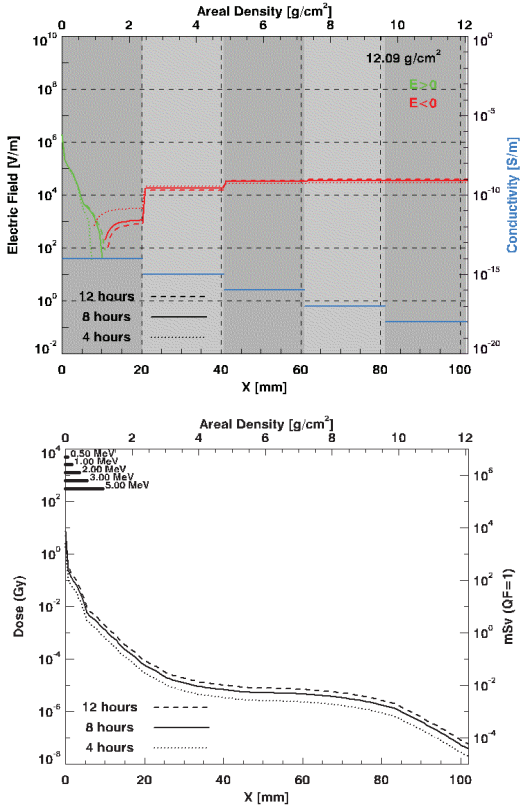
NUMIT 1-D ("numerical iteration") Codes

Originally developed by A.R. Frederickson et al (AFRL, JPL)

- Tabata algorithm fits to Monte Carlo electron transport code for radiation dose, charge deposition
- Multiple material conductivity, dielectric constant
- Input electron spectrum, monoenergetic beams, fixed flux or time series of arbitrary duration (hours to years)
- Output electric fields, charge density, currents, radiation dose rates as function of depth in material







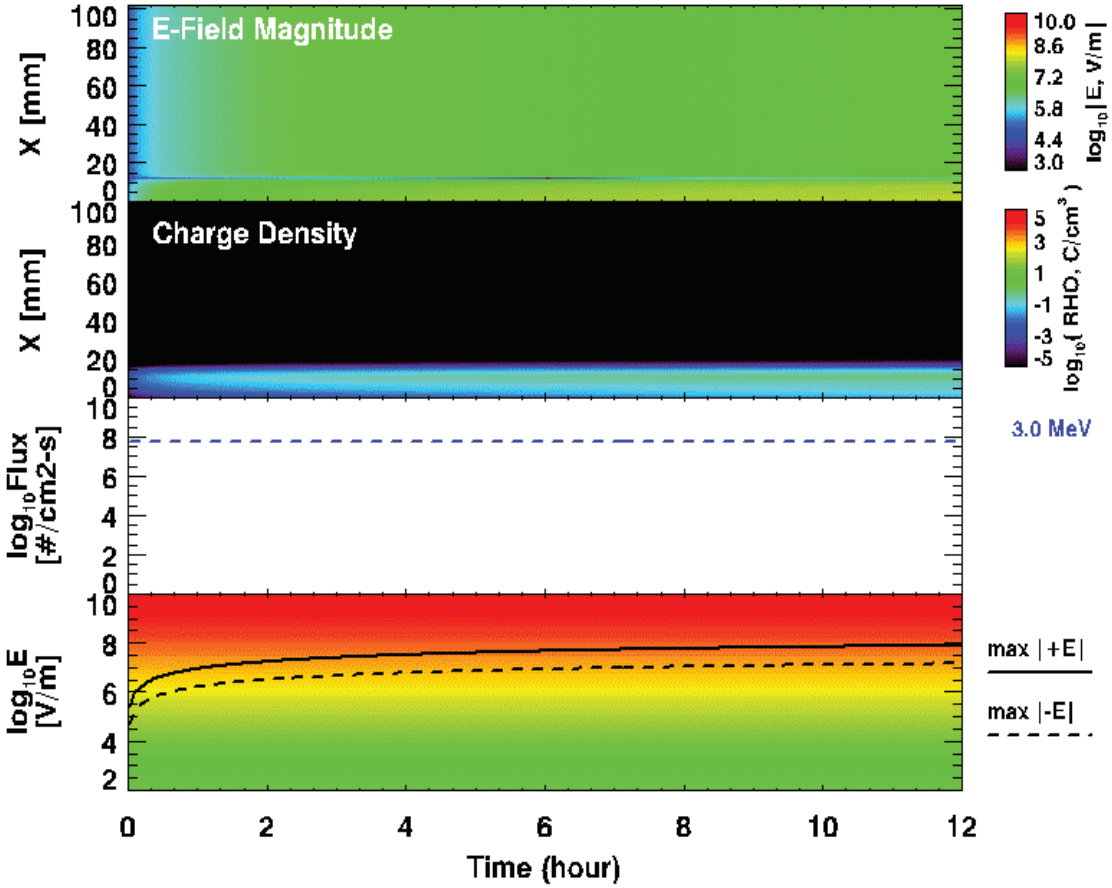
3 MeV electrons on PMMA

Charging beam

- 3 MeV electrons
- 0.01 nA/cm^2

Material

- PMMA (acrylic)
- Z=6, A=12
- ~10 cm thick
- $\sigma \sim 1 \times 10^{-16}$ S/m
- $\kappa = 3.71$
- $\rho = 1.19$ g/cm^3



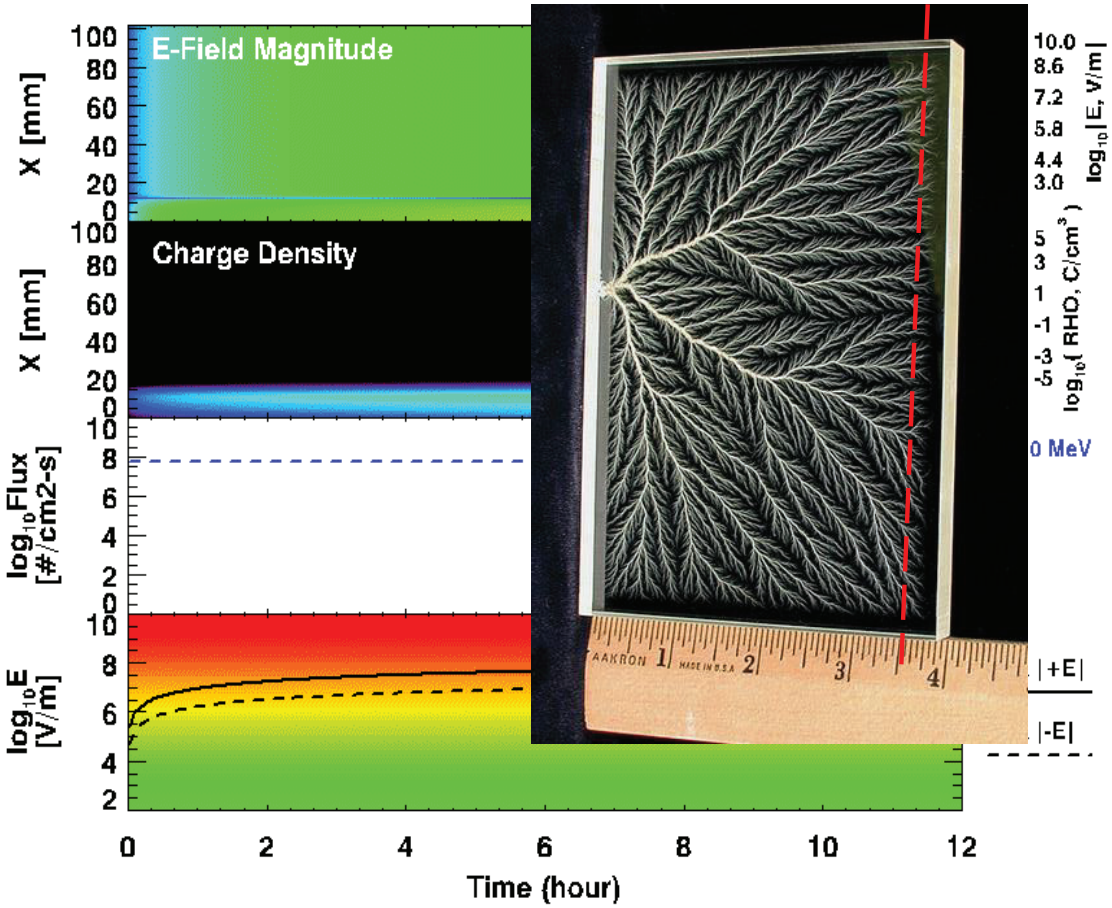
3 MeV electrons on PMMA

Charging beam

- 3 MeV electrons
- 0.01 nA/cm^2

Material

- PMMA (acrylic)
- Z=6, A=12
- ~10 cm thick
- $\sigma \sim 1 \times 10^{-16}$ S/m
- $\kappa = 3.71$
- $\rho = 1.19$ g/cm^3



3 MeV electrons on PMMA

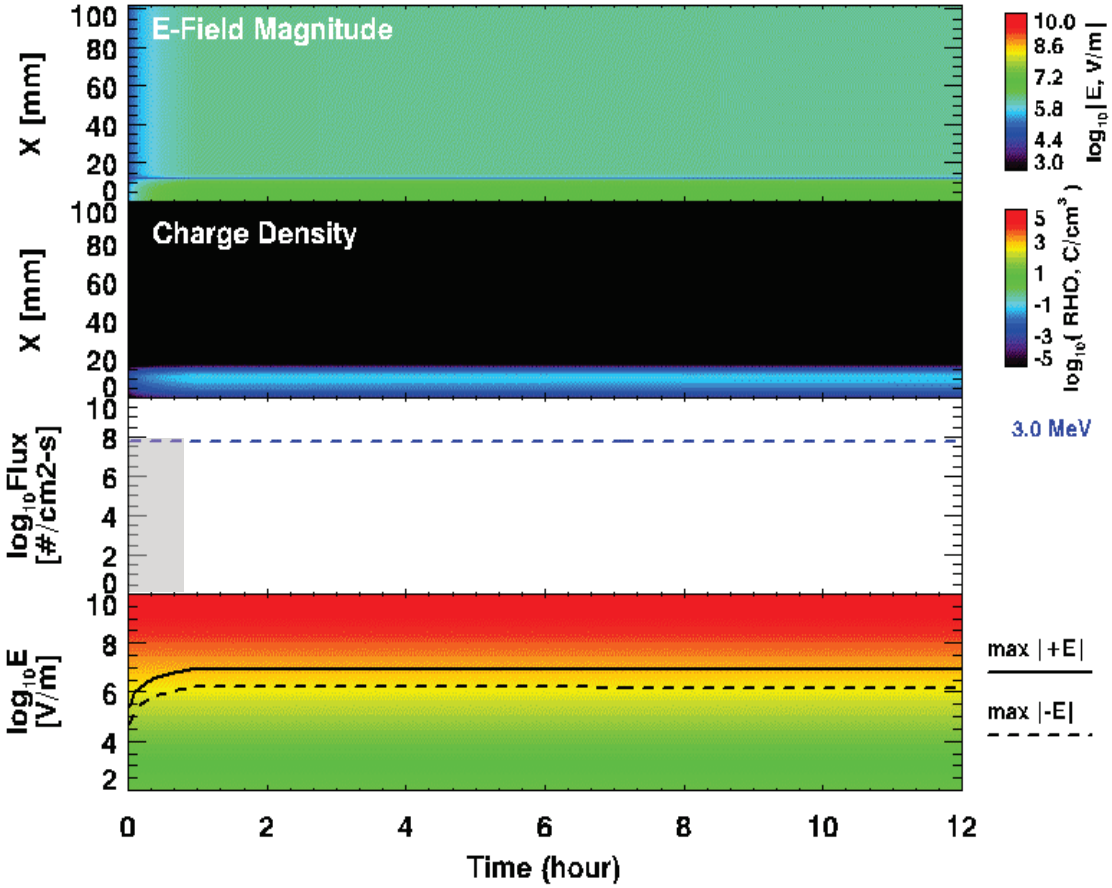
Charging beam

- 3 MeV electrons
- 0.01 nA/cm^2

Material

- PMMA (acrylic)
- Z=6, A=12
- ~10 cm thick
- **$\sigma \sim 1 \times 10^{-14}$ S/m**
- $\kappa = 3.71$
- $\rho = 1.19$ g/cm^3

- **Electron beam off at 1 hour**
- **Little effect on charge density, field since $\tau \sim \kappa\varepsilon_0/\sigma = 91$ hours**



3 MeV electrons on PMMA

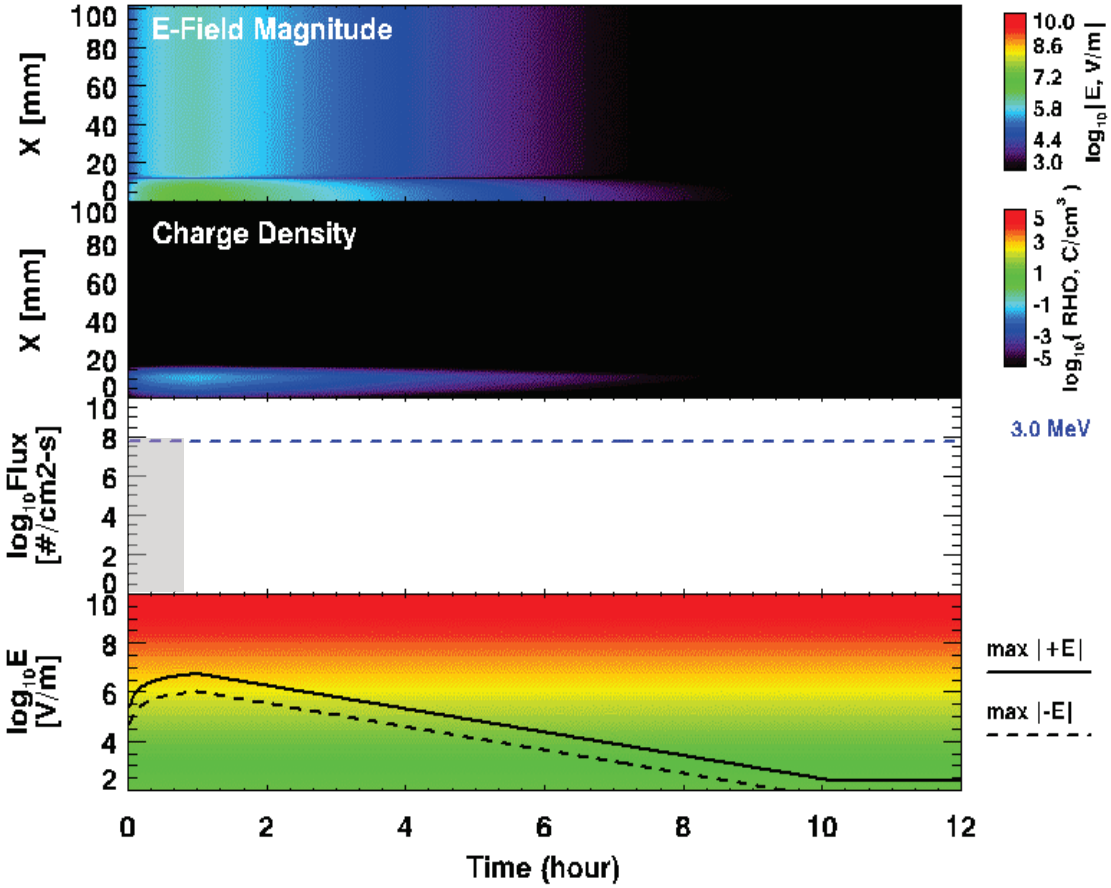
Charging beam

- 3 MeV electrons
- 0.01 nA/cm^2

Material

- PMMA (acrylic)
- Z=6, A=12
- ~10 cm thick
- **$\sigma \sim 1 \times 10^{-14}$ S/m**
- $\kappa = 3.71$
- $\rho = 1.19$ g/cm^3

- **Electron beam off at 1 hour**
- **Charge density, field decay since $\tau \sim \kappa\varepsilon_0/\sigma = 0.91$ hours**



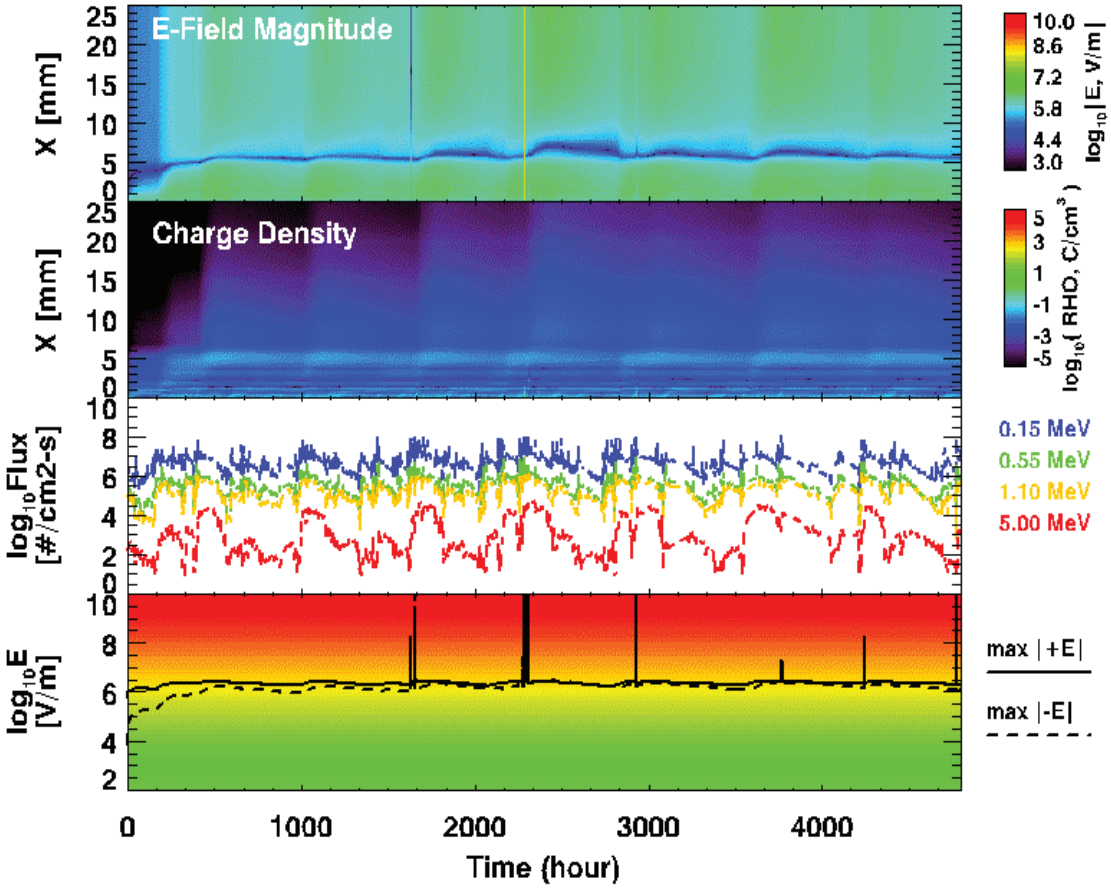
PMMA: Geostationary Orbit, 200 Days

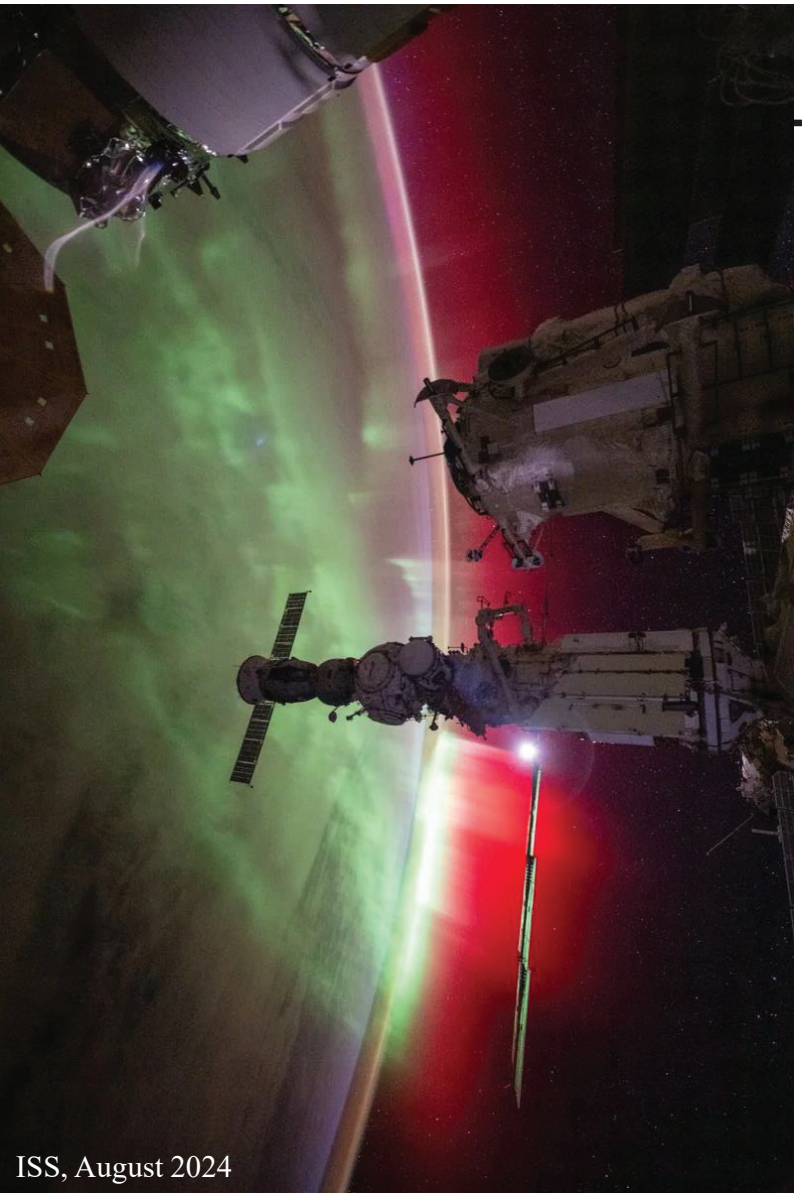
Charging current

- Energy, flux from GEO electron measurements
  - LANL-01A SOPA +ESA

Material

- PMMA
- Z=6, A=12
- ~2.5 cm thick
- $\sigma \sim 1 \times 10^{-17}$ S/m
- $\kappa = 2.00$
- $\rho = 1.0$ g/cm^3





ISS, August 2024

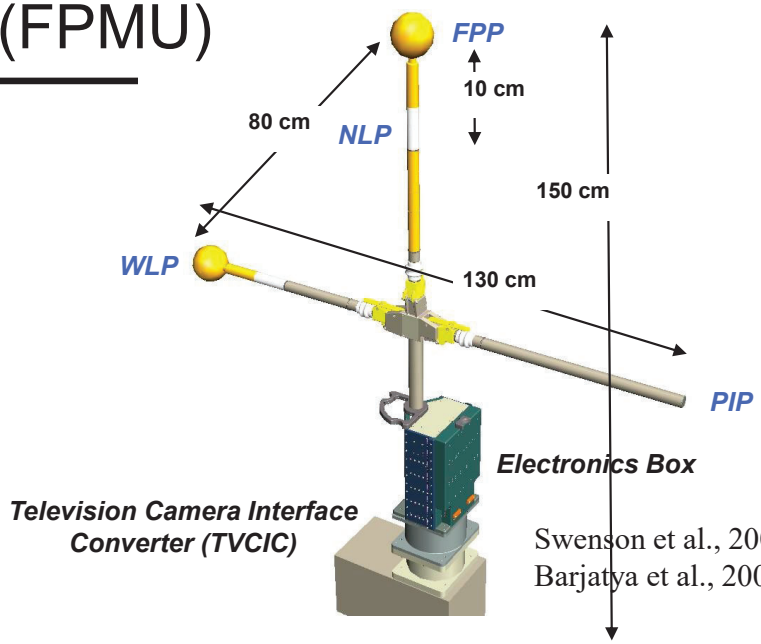
Questions?

Floating Potential Measurement Unit (FPMU)

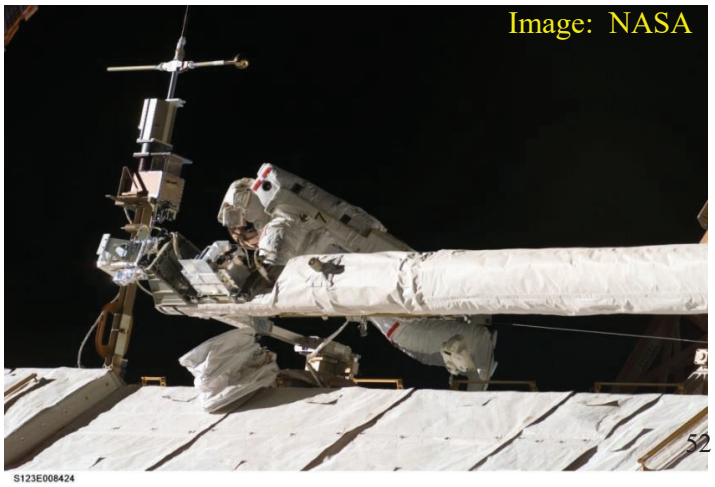
- FPMU is a suite of four plasma instruments originally deployed on the ISS in August of 2006, new instrument deployed September 2021
  - Narrow Langmuir Probe (NLP) 1 Hz Ne, Te, Ni, Vf, Vp
  - Wide Langmuir Probe (WLP) 1 Hz Ne, Te, Ni, Vf, Vp
  - Floating Potential Probe (FPP) 128 Hz Vf
  - Plasma Impedance Probe (PIP) 1 Hz Ne

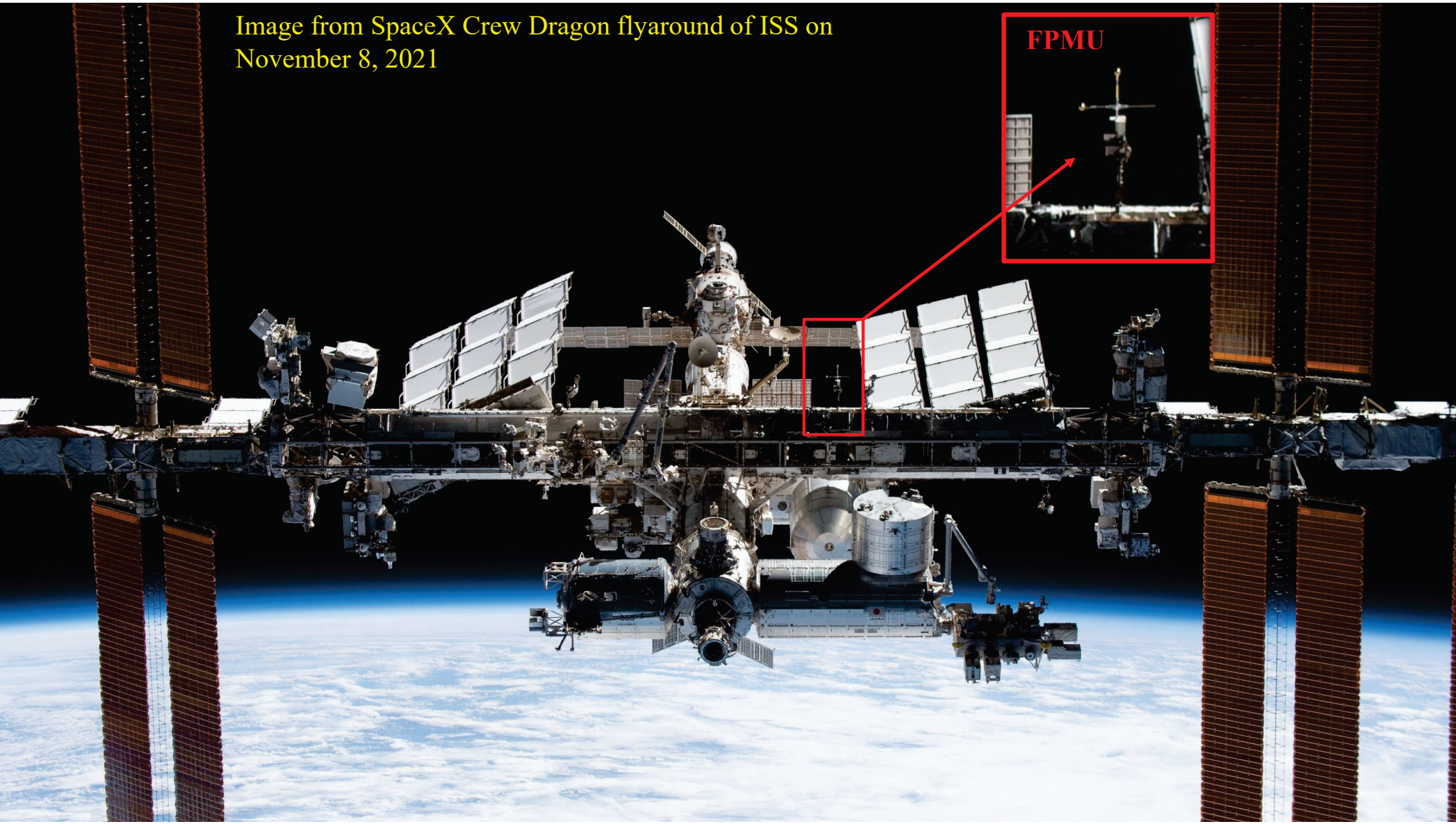
- Primary use is ISS engineering:
  - Characterize US high-voltage (160 V) solar array interactions with plasma environment.
  - Evaluate extravehicular activity plasma hazard environments and vehicle charging.
  - Validate the Plasma Interaction Model used to compute ISS frame potentials.
  - Anomaly investigations.

- Secondary use is ionospheric science applications:
  - Collaborations with ISS science payloads, other spacecraft, and ground-based ionosphere observations.
  - Support studies of the topside ionosphere near electron density peak.
  - Data provided to science community through Goddard Space Flight Center's (GSFC's) Space Physics Data Facility (SPDF).
  - Auroral charging and ISS space weather interactions.
  - Characterize geophysical events and spacecraft plasma interactions.



Swenson et al., 2003; Barjatya et al., 2009




Image from SpaceX Crew Dragon flyaround of ISS on November 8, 2021
FPMU